USGS
science for a changing world

Strontium Isotopic Composition of Paleozoic Carbonate Rocks in the Nevada Test Site Vicinity, Clark, Lincoln, and Nye Counties, Nevada, and Inyo County, California

Data Series 280

U.S. Department of the Interior
U.S. Geological Survey

Strontium Isotopic Composition of Paleozoic Carbonate Rocks in the Nevada Test Site Vicinity, Clark, Lincoln, and Nye Counties, Nevada, and Inyo County, California

By James B. Paces, Zell E. Peterman, Kiyoto Futa, Thomas A. Oliver, and Brian D. Marshall

Data Series 280

U.S. Department of the Interior
U.S. Geological Survey

U.S. Department of the Interior
DIRK KEMPTHORNE, Secretary

U.S. Geological Survey
Mark D. Myers, Director

U.S. Geological Survey, Reston, Virginia: 2007

Suggested citation:
Paces, J.B., Peterman, Z.E., Futo, Kiyoto, Oliver, T.A., and Marshall, B.D., 2007, Strontium isotopic composition of paleozoic carbonate rocks in the Nevada Test Site vicinity, Clark, Lincoln, and Nye Counties, Nevada, and Inyo County, California: U.S. Geological Survey Data Series 280, 42 p.

Contents

Figures

Figures—Continued

Tables

Conversion Factors, Datum, Definitions, and Abbreviations and Acronyms

Conversion Factors

Multiply	By	To obtain
centimeter (cm)	0.3937	inch
gram (g)	0.03527	ounce, avoirdupois
kilometer (km)	0.6214	mile
meter (m)	3.281	foot
meter (m)	1.094	yard
millimeter (mm)	0.03937	inch
square kilometer (km^2)	0.6124	square mile

Temperature in degrees Celsius (°C) may be converted to degrees Fahrenheit (°F) as follows:

$$°F=(1.8×°C)+32.$$

Datum

Horizontal coordinates convention: Horizontal coordinates, given in meters, are referenced to the Universal Transverse Mercator (UTM) system of Easting (X coordinate) and Northing (Y coordinate) distances within Zone 11 and are based on the North American datum of 1927 (NAD27).

Definitions

Isotope notation conventions: Strontium isotopic compositions are given as both atomic ratios of $^{87}Sr/^{86}Sr$ as well as delta strontium-87 ($\delta^{87}Sr$) calculated using the formula:

$$\delta^{87}Sr = [(^{87}Sr/^{86}Sr_{sample}/^{87}Sr/^{86}Sr_{msw})-1]×1000,$$

where $^{87}Sr/^{86}Sr_{msw}$ is the value for modern sea water (msw) of 0.70920, and the resulting value is in parts per thousand or per mil (‰). In addition, delta strontium-87 can be calculated using the value for seawater $^{87}Sr/^{86}Sr$ at the time of rock deposition and is designated as $\delta^{87}Sr_t$.

Geochronological conventions: Abbreviations used to designate geologic time in this report are mega-annum (Ma) to specify a specific time in millions of years before the present, and millions of years (m.y.) to specify the duration of a remote time interval.

Units of concentration: Concentrations of chemical constituents measured in unknown rock samples are given in weight percent (parts per hundred, abbreviated by wt. %) for major elements in the form of oxides, and micrograms per gram (parts per million, abbreviated by µg/g) for trace elements. Concentrations of acids used to digest the carbonate fraction of rock samples are given in Molarity units equal to the number of moles of a solute per liter of solvent (abbreviated as M).

Abbreviations and Acronyms

Abbreviation	Chemical Species
Al_2O_3	aluminum oxide, or alumina
Ba	barium
CaO	calcium oxide
$CaCO_3$	calcium carbonate (calcite)
Ce	cerium
La	lanthanum
MgO	magnesium oxide
MnO	manganese oxide
Nb	niobium
SiO_2	silicon dioxide
Rb	rubidium
Sr	strontium
Th	thorium
U	uranium
Y	yittrium
Zr	zirconium

Acronym	Definition
DOE	U.S. Department of Energy
ICP-MS	Inductively coupled plasma mass spectrometry
LCA	lower carbonate aquifer
NTS	Nevada Test Site
SRM	Standard Reference Material
USGS	U.S. Geological Survey
XRF	X-ray fluorescence

Strontium Isotopic Composition of Paleozoic Carbonate Rocks in the Nevada Test Site Vicinity, Clark, Lincoln, and Nye Counties, Nevada, and Inyo County, California

By James B. Paces, Zell E. Peterman, Kiyoto Futa, Thomas A. Oliver, and Brian D. Marshall

Abstract

Ground water moving through permeable Paleozoic carbonate rocks represents the most likely pathway for migration of radioactive contaminants from nuclear weapons testing at the Nevada Test Site, Nye County, Nevada. The strontium isotopic composition ($^{87}Sr/^{86}Sr$) of ground water offers a useful means of testing hydrochemical models of regional flow involving advection and reaction. However, reaction models require knowledge of $^{87}Sr/^{86}Sr$ data for carbonate rock in the Nevada Test Site vicinity, which is scarce. To fill this data gap, samples of core or cuttings were selected from 22 boreholes at depth intervals from which water samples had been obtained previously around the Nevada Test Site at Yucca Flat, Frenchman Flat, Rainier Mesa, and Mercury Valley. Dilute acid leachates of these samples were analyzed for a suite of major- and trace-element concentrations (MgO, CaO, SiO_2, Al_2O_3, MnO, Rb, Sr, Th, and U) as well as for $^{87}Sr/^{86}Sr$. Also presented are unpublished analyses of 114 Paleozoic carbonate samples from outcrops, road cuts, or underground sites in the Funeral Mountains, Bare Mountain, Striped Hills, Specter Range, Spring Mountains, and ranges east of the Nevada Test Site measured in the early 1990's. These data originally were collected to evaluate the potential for economic mineral deposition at the potential high-level radioactive waste repository site at Yucca Mountain and adjacent areas (Peterman and others, 1994). Samples were analyzed for a suite of trace elements (Rb, Sr, Zr, Ba, La, and Ce) in bulk-rock powders, and $^{87}Sr/^{86}Sr$ in partial digestions of carbonate rock using dilute acid or total digestions of silicate-rich rocks. Pre-Tertiary core samples from two boreholes in the central or western part of the Nevada Test Site also were analyzed. Data are presented in tables and summarized in graphs; however, no attempt is made to interpret results with respect to ground-water flow paths in this report. Present-day $^{87}Sr/^{86}Sr$ values are compared to values for Paleozoic seawater present at the time of deposition. Many of the samples have $^{87}Sr/^{86}Sr$ compositions that remain relatively unmodified from expected seawater values. However, rocks underlying the northern Nevada Test Site as well as rocks exposed at Bare Mountain commonly have elevated $^{87}Sr/^{86}Sr$ values derived from post-depositional addition of radiogenic Sr most likely from fluids circulating through rubidium-rich Paleozoic strata or Precambrian basement rocks.

Introduction

The Nevada Test Site (NTS), occupying approximately 3,500 km^2 in southern Nevada (fig. 1), has been the primary site for underground testing of nuclear weapons by the United States since the late 1950's. Radioactive byproducts have been emplaced above and below the regional water table as a result of this testing (Laczniak and others, 1996, p. 2). In an effort to understand the movement of these radioactive contaminants (radionuclides) away from areas of underground testing, the U.S. Department of Energy (DOE) has established an Environmental Restoration Program to investigate the hydrologic pathways and travel times associated with regional ground-water flow beneath the NTS and vicinity (U.S. Department of Energy, 1991, p. 2). Fractures in Middle Cambrian through Devonian limestones and dolomites constituting the regional lower carbonate aquifer (LCA) are the most likely pathways for the transport of radioactive nuclides (Winograd and Thordarson, 1975, p. 119; Laczniak and others, 1996, p. 15).
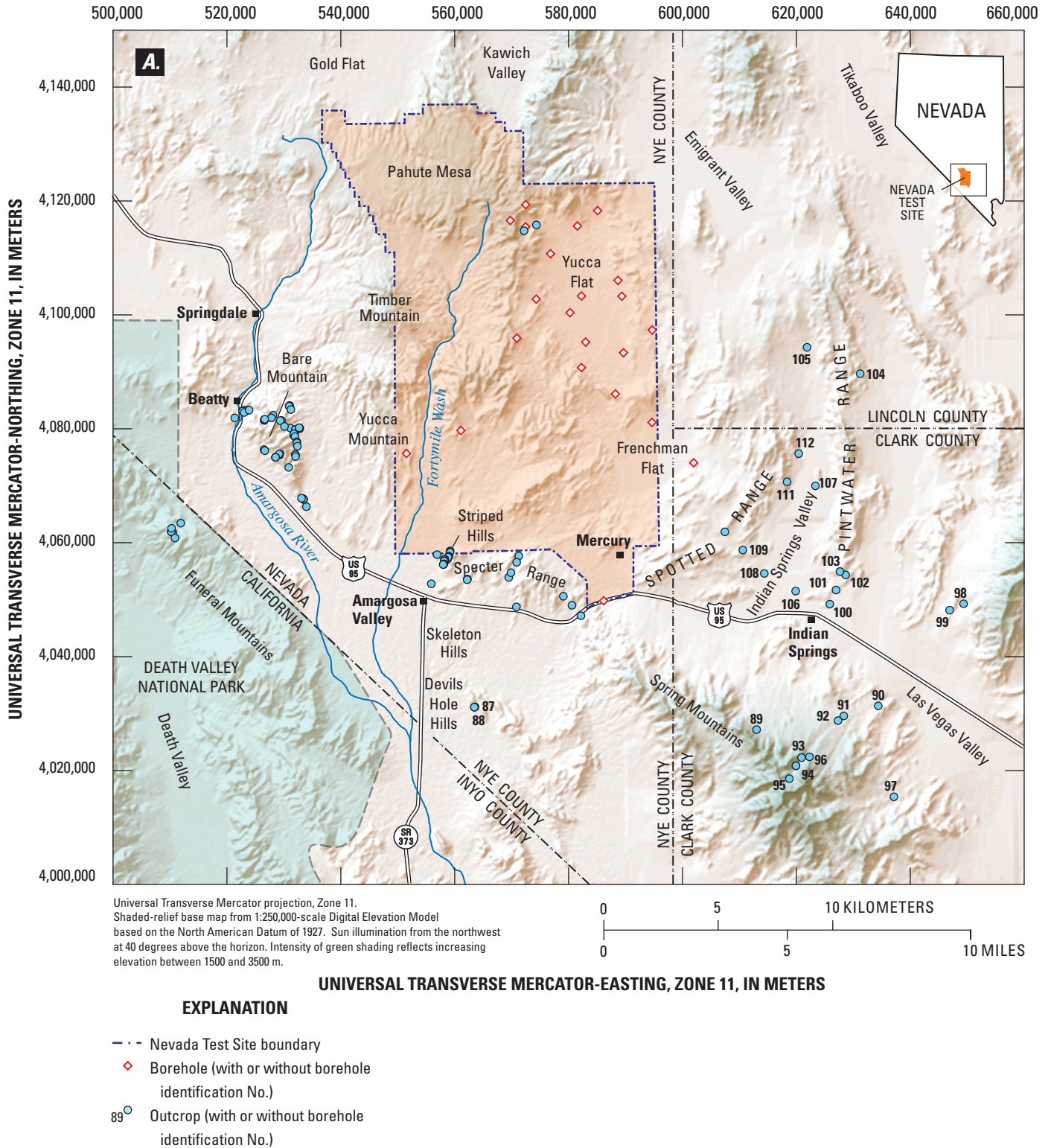
Universal Transverse Mercator projection, Zone 11.
Shaded-relief base map from 1:250,000-scale Digital Elevation Model
based on the North American Datum of 1927. Sun illumination from the northwest
at 40 degrees above the horizon. Intensity of green shading reflects increasing
elevation between 1500 and 3500 m.

UNIVERSAL TRANSVERSE MERCATOR-EASTING, ZONE 11, IN METERS

EXPLANATION

– - · – Nevada Test Site boundary

◇   Borehole (with or without borehole
       identification No.)

89○   Outcrop (with or without borehole
       identification No.)

Figure 1.   Location of borehole and outcrop samples from (*A*) the Nevada Test Site region; (*B*) in and adjacent to the Nevada Test Site; and (*C*) Bare Mountain and the Funeral Mountains, Clark, Lincoln, and Nye Counties, Nevada, and Inyo County, California. Boreholes and outcrop sites without labels in figure 1*A* are identified in figures 1*B* or 1*C*. Map numbers for outcrop samples are keyed to tables 4 and 6.

Figure 1. Continued.

Figure 1.   Continued.
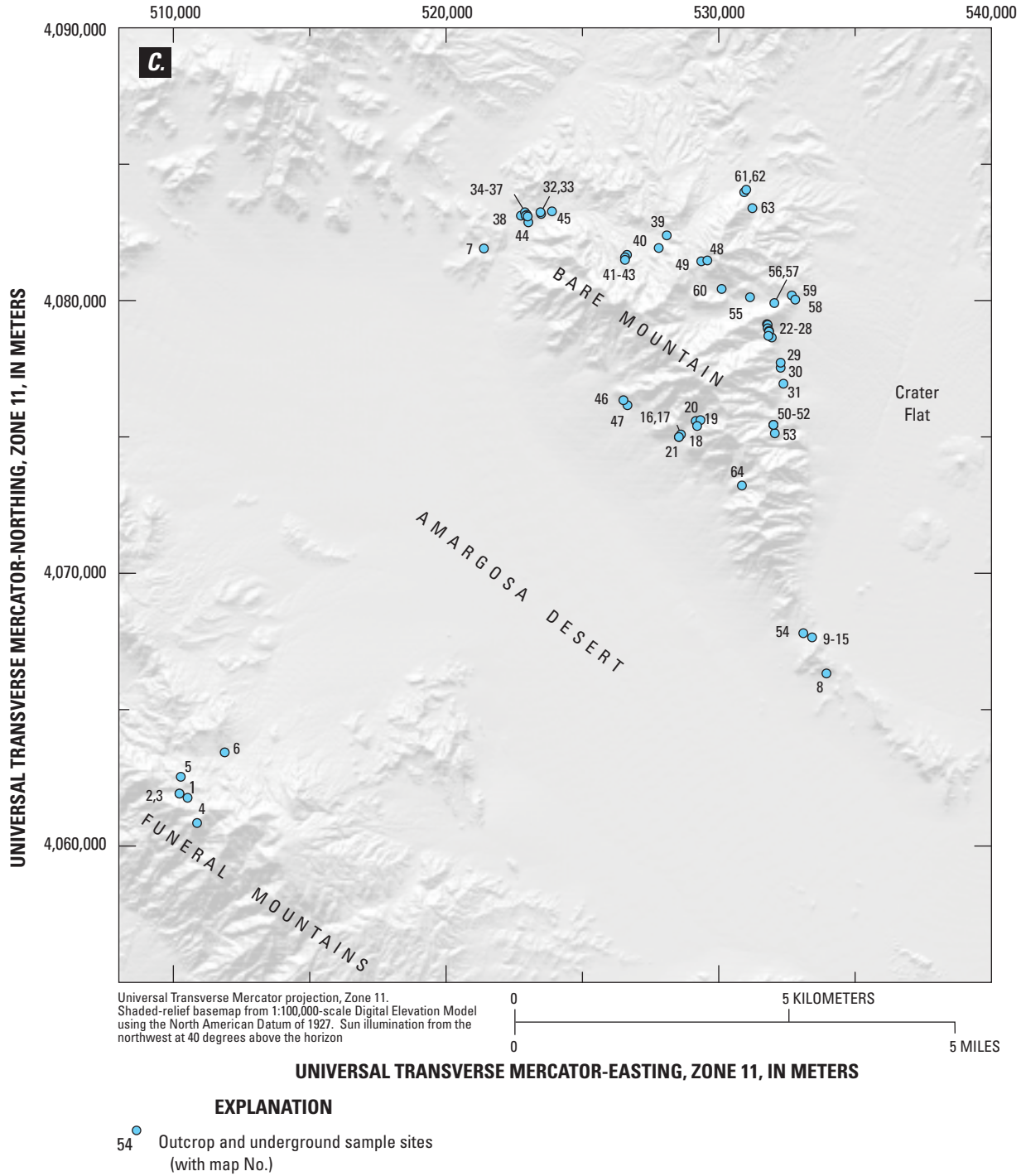
Geochemical and isotopic data from ground-water samples are being used to evaluate possible ground-water flow paths in the DOE Environmental Restoration Program (Thomas and others, 2002; Hershey and others, 2005; Rose and others, 2006; Farnham and others, 2006). Conservative tracers (isotopes or elements that undergo negligible modification by water-rock interaction) typically are used to delineate ground-water flow paths and evaluate mixing of water masses from upgradient sources. These tracers are combined with other dissolved constituents in advection-reaction geochemical modeling (NETPATH, PHREEQC) to evaluate chemical evolution along postulated ground-water flow paths. However, to understand the potential contributions of rock and mineral constituents, chemical compositions of aquifer components are required as inputs in geochemical models. Isotope tracers of geochemical processes can help discriminate between alternative flow models whose solutions may remain non-unique based on chemical concentrations alone. Like other chemical constituents, an understanding of the range of compositions in both water and rock is required for constraining flow paths and for evaluating possible aquifer-water interactions.

Use of Strontium Isotopic Composition as a Ground-Water Tracer

The isotopic composition of strontium ($^{87}Sr/^{86}Sr$) can be used as a natural tracer of ground-water flow because the strontium ion (Sr^{+2}) is soluble in aqueous solutions at levels allowing high-precision isotope measurement, because variations in rubidium-to-strontium (Rb/Sr) ratios in rocks of different type and petrogenetic origin result in distinctive $^{87}Sr/^{86}Sr$ ground-water signatures, and because fractionation of heavy radiogenic isotopes (^{87}Sr from ^{86}Sr) is negligible for geologic processes (Peterman and Stuckless, 1992; McNutt, 2000). However, unlike conservative tracers, $^{87}Sr/^{86}Sr$ values can be modified along ground-water flow paths by reaction with the aquifer rock. Studies have shown that Sr dissolved in ground water may not be in isotopic equilibrium with the aquifer through which it flows (Peterman and Stuckless, 1992, and references therein). This disequilibrium commonly provides important insight into the ground-water flow system for which conceptual models may otherwise be oversimplified. For example, in several carbonate aquifer studies, $^{87}Sr/^{86}Sr$ ratios in ground-water samples are larger than those of the aquifer rock (Chaudhuri and others, 1987; Banner and others, 1989, p. 396; McKenna and others, 1992; Peterman and others, 1992, p. 827; Frost and Toner, 2004). This disequilibrium requires ground-water contributions from associated Precambrian rocks having higher $^{87}Sr/^{86}Sr$ signatures, but which typically were considered to be impermeable.

The behavior of Sr and $^{87}Sr/^{86}Sr$ in ground-water flow systems depends on numerous factors including length of flow path, water-to-rock mass ratio, chemical reaction rates, Sr concentration and $^{87}Sr/^{86}Sr$ in solid and fluid phases, flow velocity, advective fluid mixing, dispersion, and ion exchange (Johnson and DePaolo, 1994, 1997). In aquifers dominated by fracture flow, the Sr isotopic composition of water is less likely to be modified by changes in rock $^{87}Sr/^{86}Sr$ values along a flow path than in aquifers dominated by matrix flow because of faster flow velocities, larger water-to-rock mass ratios, and slower reaction rates (Johnson and others, 2000). Therefore, in aquifers dominated by fracture flow or high permeability matrix flow, such as alluvium, Sr may be useful as a tracer of water from upgradient sources (Johnson and DePaolo, 1994, p. 1576), at least at path lengths commensurate with the scale of the NTS.

Chemical processes resulting in nonconservative behavior of Sr in ground water affect Sr concentrations to a greater extent than $^{87}Sr/^{86}Sr$ values. Losses of Sr from solution due to sorption and mineral precipitation will not change the $^{87}Sr/^{86}Sr$ ratio in the remaining fluid. Furthermore, desorption or cation exchange from reactive mineral surfaces along flow paths may not significantly affect $^{87}Sr/^{86}Sr$ values if the dynamics of flow and sources of Sr have remained unchanged over long periods (steady-state flow conditions). In contrast, rock dissolution can add Sr containing very different isotopic compositions to solution, particularly if ground water that is unsaturated, with respect to calcite or dolomite, flows into the LCA.

Need for Strontium Isotopic Compositions of Paleozoic Carbonate Rock Data

Use of $^{87}Sr/^{86}Sr$ as a tracer in advection-reaction geochemical models of ground-water flow in the LCA requires knowledge of rock Sr concentrations and $^{87}Sr/^{86}Sr$ compositions. The structures of minerals constituting marine carbonate deposits result in rocks with relatively high Sr concentrations and low Rb concentration. Therefore, the $^{87}Sr/^{86}Sr$ values inherited from seawater will not change appreciably with time due to the decay of ^{87}Rb. However, previous studies demonstrated that at least some Paleozoic carbonate rocks in the NTS vicinity have nonmarine $^{87}Sr/^{86}Sr$ compositions indicating that radiogenic ^{87}Sr from crustal sources was introduced into the carbonate rocks at some time in the past (Peterman and others, 1994; J. Kenneally, Lawrence Livermore National Laboratory, written commun., 1995). These studies indicate that Paleozoic carbonate rocks at the NTS can have a much wider range of $^{87}Sr/^{86}Sr$ values that are more radiogenic than values derived from a seawater origin.

Ground water flowing through the LCA on the east side of the NTS commonly has $^{87}Sr/^{86}Sr$ values that are greater than values expected from seawater sources (Hershey and others, 2005; Farnham and others, 2006). Advection-reaction geochemical models of ground-water evolution between sample sites commonly require small amounts of mineral dissolution that would likely affect the $^{87}Sr/^{86}Sr$ of dissolved Sr in the water. However, because $^{87}Sr/^{86}Sr$ compositions of most carbonate rocks on the NTS generally are not available, the influence of water-rock reaction during chemical evolution along flow paths cannot be evaluated effectively. Therefore, it is necessary to better constrain rock $^{87}Sr/^{86}Sr$ values present along potential flow paths to more reliably utilize $^{87}Sr/^{86}Sr$ as a ground-water tracer.

Description of Study Area

Because ground-water flow through the LCA represents the most likely scenario for transporting radionuclides beyond the eastern and southern boundaries of the NTS, characterization of $^{87}Sr/^{86}Sr$ in Paleozoic carbonate rocks constitutes the focus of this study. A small number of older carbonate rocks as well as a few samples of Paleozoic silicate rocks are also included. Most rocks constituting the LCA were deposited as chemical precipitates from Paleozoic seawater. Because this reservoir is well mixed on a global scale by vertical and lateral circulation patterns, its Sr isotope evolution has been well documented by examining samples from many other areas. Both the stratigraphy of pre-Tertiary rocks and the evolution of seawater $^{87}Sr/^{86}Sr$ are described in the following sections.

Pre-Tertiary Stratigraphy

Pre-Tertiary rocks of southeastern Nevada consist of a thick sequence of older (Neoproterozoic to Devonian in age) shallow-water marine sediments deposited in a miogeoclinal (passive continental shelf) environment and younger (Devonian to Mississippian in age) marine sediments deposited in a foreland basin along the Cordilleran continental margin. A generalized stratigraphic succession of the approximately 11,500-m-thick sequence of pre-Tertiary rocks present on the NTS is shown in figure 2. The summary presented below is compiled from more detailed descriptions presented by Burchfiel (1964), Barnes and Christiansen (1967), Stewart and Poole (1974), Winograd and Thordarson (1975), Monsen and others (1992), Laczniak and others (1996), Trexler and others (1996; 2003), Slate and others (1999), and Page and others (2005). Age estimates for stratigraphic units from the NTS and surrounding areas are listed in table 1.

The oldest sedimentary rocks on the NTS consist of a 2,800-m-thick series of Neoproterozoic and lower Cambrian deposits dominated by marine clastic sediments (quartzite, arkose, siltstone, and shale/argillite). Silty carbonate units, such as the Noonday Dolomite and dolomitic units in the Wood Canyon and Johnnie Formations, are present locally in this sequence. The well-cemented to moderately metamorphosed rocks of this sequence generally are considered to be poor transmitters of ground-water flow and constitute the lower clastic confining unit of Winograd and Thordarson (1975). The Lower-to-Middle Cambrian Carrara Formation contains siltstone and shale with thin, but persistent, limestone beds that become more common up-section. These time-transgressive lithologic changes reflect the regional transition to a depositional environment dominated by marine carbonate sedimentation.

The 5,200-m-thick section of Middle Cambrian through Devonian rocks is composed of marine limestones and dolomites with minor interbeds of sandy or silty clastic units (Barnes and Christiansen, 1967; Stewart and Poole, 1974; Trexler and others, 1996, 2003; Slate and others, 1999). Aquifer tests indicate very high degrees of water transmissivity through these units due to extensive secondary permeability along a well-connected network of solution-enhanced fractures, faults, and breccias (Winograd and Thordarson, 1975, p. 117; Laczniak and others, 1996). Collectively, these rocks constitute the LCA and provide the main pathways for ground-water flow between Tertiary basins. Because the few clastic units within this sequence (Dunderberg Shale Member of the Nopah Formation, the Ninemile Formation of the Pogonip Group, and the Eureka Quartzite) are thin and structurally disrupted, they do not constitute regionally effective confining units, though they may impede flow locally (Laczniak and others, 1996, p. 15).

Mississippian strata overlying Devonian and older carbonates of the LCA are mostly clastic rocks (conglomeritic sandstone, siltstone, shale, bioclastic limestone, and rare quartzite) to the west of Yucca Flat and carbonate to the east of the NTS (Winograd and Thordarson, 1975, p. 9; Trexler and others, 1996, 2003). These rocks reflect a change from sedimentation along a passive continental margin to clastic-dominated depositional environments in foreland basins associated with convergent tectonics of the Antler orogeny (Poole, 1974; Cole and others, 1997; Cole and Cashman, 1999; Trexler and others, 2003). Up to 3,000 m of predominantly synorogenic siliciclastic rocks constitute the Late Devonian to Middle Mississippian Eleana Formation and laterally equivalent Gap Wash Formation as well as the overlying Late Mississippian Chainman Shale/Captain Jack Formations (Cole and Cashman, 1999; Trexler and others, 2003).

Rock system	Stratigraphic unit		Abbreviation	Hydrogeologic unit
Tertiary	Valley-fill deposits			Alluvial aquifer
	Volcanic rocks			Volcanic aquifers and confining units
Lower Permian & Pennsylvanian	Tippipah Limestone		PPt	Upper carbonate-rock aquifer
Mississippian and upper Devonian	Chainman Shale		Mc	Upper clastic confining unit
	Gap Wash Formation Eleana Formation		MDg MDe	
Devonian	Guilmette Formation		Dg	Lower carbonate-rock aquifer
	Simonson Dolomite		Dsi	
	Sevy Dolomite		Dsv	
Devonian and Silurian	Lone Mountain Dolomite		DSlm	
Silurian	Roberts Mountains Formation		Sr	
	Laketown Dolomite		Sl	
Ordovician	Ely Springs Dolomite		Oes	
	Eureka Quartzite		Oeq	
	Pogonip Group	Antelope Valley Limestone	Op-av	
		Ninemile Formation	Op-n	
		Goodwin Limestone	Op-g	
Cambrian	Nopah Formation	Smoky Member	€n-s	
		Halfpint Member	€n-h	
		Dunderberg Shale Member	€n-d	
	Bonanza King Formation	Banded Mountain Member	€bb	
		Papoose Lake Member	€bp	
	Carrara Formation	Upper part	€c-u	
		Lower part	€c-l	Lower clastic confining unit
Cambrian and Neoproterozoic	Wood Canyon Formation		€Zw	
Neoproterozoic	Stirling Quartzite		Zs	
	Johnnie Formation		Zj	
	Noonday Dolomite		Zn	Not classified

Figure 2.   Principal pre-Tertiary stratigraphic units and associated hydrogeologic units sampled in Nevada Test Site boreholes, Nye County, Nevada.

Table 1.   Ages and seawater strontium isotopic composition ($^{87}Sr/^{86}Sr$) of stratigraphic units present in the Nevada Test Site region, southern Nevada.

[**Stratigraphic units and epochs** are from the U.S. Geological Survey Geologic Names Lexicon database (http://ngmdb.usgs.gov/Geolex/geolex_home.html). Age assignments are based on the time scale of Young and Laurie (1996), which McArthur and others (2001) used to construct the Paleozoic seawater curve (fig. 3). Maximum, minimum, and mean Sr isotopic compositions are determined from values shown in figure 3 averaged over the time period given. Age ranges are given in millions of years before present (m.y.)]

Symbol	Stratigraphic unit	Epoch	Age range (m.y.)	Minimum $^{87}Sr/^{86}Sr$	Maximum $^{87}Sr/^{86}Sr$	Mean $^{87}Sr/^{86}Sr$
PPt	Tippipah Limestone	Pennsylvanian and Early Permian	270–325	0.7073	0.7084	0.7080
PMb	Bird Spring Formation–undivided	Late Mississippian and Early Permian	270–340	.7073	.7084	.7079
PMbl	Bird Spring Formation–lower member	Late Mississippian and Early Permian	270–340	.7073	.7084	.7080
Mm	Monte Cristo group	Early and Late Mississippian	325–354	.7077	.7084	.7079
Mc	Chainman Shale	Early and Late Mississippian	325–354	.7077	.7082	.7079
Mj	Joana Limestone	Early Mississippian	340–354	.7077	.7082	.7080
MDe	Eleana Formation	Late Devonian and Mississippian	325–369	.7077	.7083	.7080
MDg	Gap Wash Formation	Late Devonian and Mississippian	325–369	.7077	.7083	.7080
Dg	Guilmette Formation	Middle and Late Devonian	354–384	.7078	.7083	.7080
Df	Fluorspar Canyon Formation	Middle Devonian	369–384	.7078	.7079	.7079
Dsi	Simonson Dolomite	Middle Devonian	369–384	.7078	.7079	.7079
Dtc	Rocks of Tarantula Canyon	Devonian	354–410	.7078	.7088	.7082
Dsv	Sevy Dolomite	Early and Middle Devonian	369–410	.7078	.7088	.7082
Du	Undifferentiated rocks of Devonian in age	Devonian	354–410	.7078	.7088	.7082
DSlm	Lone Mountain Dolomite	Late Silurian and Early Devonian	384–420	.7079	.7088	.7085
DSu	Undifferentiated rocks of Devonian or Silurian age	Devonian or Silurian	354–434	.7078	.7088	.7083
Sr	Roberts Mountains Formation	Silurian	410–434	.7080	.7088	.7084
Sl	Laketown Dolomite	Silurian	410–434	.7080	.7088	.7084
Oes	Ely Springs Dolomite	Late Ordovician	434–459	.7079	.7085	.7081
Op	Pogonip Group	Late Cambrian and MiddleOrdovician	459–498	.7084	.7091	.7089
Op-av	Antelope Valley Limestone of Pogonip Group	Early and Middle Ordovician	459–490	.7084	.7091	.7089
Op-g	Goodwin Limstone of Pogonip Group	Early Ordovician and LateCambrian	470–498	.7089	.7091	.7090
Ou	Undifferentiated rocks of Ordovician age	Ordovician	434–490	.7079	.7091	.7085

Although silty carbonate beds present in the Late Mississippian Captain Jack Formation (and, to a lesser extent, Chainman Shale) reflect a return to shallow-water marine environments, the thick siliciclastic sediments have low permeability and form the upper clastic confining unit in western Yucca Flat and Jackass Flat that isolates most regional ground-water flow in the LCA (Winograd and Thordarson, 1975, p. 43). Approximately 1,100 m of Pennsylvanian to early Permian Tippipah Limestone are preserved in two localities in the central NTS that unconformably overlie muddy shelf deposits of the Chainman Shale (Cole and Cashman, 1999). Winograd and Thordarson (1975, p. 30) included these rocks in the upper-carbonate-rock aquifer, but recognized their restricted distribution within the saturated zone and the limited role of the upper carbonate aquifer in regional ground-water movement. East of the NTS, the upper clastic confining unit is not present and Paleozoic carbonate rocks, regardless of age, form a single regional carbonate-rock aquifer (Laczniak and others, 1996, p. 15).

Table 1. Ages and seawater strontium isotopic composition (^{87}Sr/^{86}Sr) of stratigraphic units present in the Nevada Test Site region, southern Nevada.—Continued

[**Stratigraphic units and epochs** are from the U.S. Geological Survey Geologic Names Lexicon (GEOLEX) database (http://ngmdb.usgs.gov/Geolex/geolex_home.html). Age assignments are based on the time scale of Young and Laurie (1996), which McArthur and others (2001) used to construct the Paleozoic seawater curve (fig. 3). Maximum, minimum, and mean Sr isotopic compositions are determined from values shown in figure 3 averaged over the time period given. Age ranges are given in millions of years before present (m.y.)]

Symbol	Stratigraphic unit	Epoch	Age range (m.y.)	Minimum ^{87}Sr/^{86}Sr	Maximum ^{87}Sr/^{86}Sr	Mean ^{87}Sr/^{86}Sr
OCu	Undifferentiated rocks of Ordovician or Cambrian age	Ordovician or Cambrian	434–509	0.7079	0.7091	0.7086
Cn	Nopah Formation	Late Cambrian	490–498	.7091	.7092	.7091
Cn-s	Smoky Member of Nopah Formation	Late Cambrian	490–498	.7091	.7092	.7091
Cn-h	Halfpint Member of Nopah Formation	Late Cambrian	490–498	.7091	.7092	.7091
Cn-d	Dunderberg Shale Member of Nopah Formation	Late Cambrian	490–498	.7091	.7092	.7091
Cb	Bonanza King Formation	Middle and Late Cambrian	490–509	.7088	.7092	.7091
Cb-b	Banded Mountain Member of Bonanza King Formation	Late Cambrian	490–498	.7091	.7092	.7091
Cb-p	Papoose Lake Member of Bonanza King Formation	Middle Cambrian	498–509	.7090	.7092	.7090
Cu	Undifferentiated rocks of Cambrian Age	Cambrian	490–542	.7085	.7091	.7088
Cc	Carrara Formation	Early and Middle Cambrian	498–542	.7085	.7092	.7087
Cc-m	Carrara Formation-Middle Part	Early and Middle Cambrian	498–542	.7085	.7092	.7087
CZw	Wood Canyon Formation	Neoproterozoic and EarlyCambrian	509–600	.7079	.7088	.7084
CZw-u	Wood Canyon Formation-Upper Member	Early Cambrian	509–542	.7085	0.7088	.7086
CZw-l	Wood Canyon Formation-Lower Member	Neoproterozoic	542–600	.7085	.7079	.7084
Zs	Stirling Quartzite	Neoproterozoic	542–1,000	.7055	.7085	Undefined
Zs-c	Stirling Quartzite-C Member	Neoproterozoic	542–1,000	.7055	.7085	Undefined
Zs-d	Stirling Quartzite-D Member	Neoproterozoic	542–1,000	.7055	.7085	Undefined
Zj	Johnnie Formation	Neoproterozoic	542–1,000	.7055	.7085	Undefined
Zn	Noonday Dolomite	Neoproterozoic	542–1,000	.7055	.7085	Undefined
ZYb	Beck Spring Dolomite	Neoproterozoic and Mesoproterozoic	542–1,600	.7055	.7085	Undefined
ZYc	Crystal Spring Formation of Pahrump Group	Neoproterozoic and Mesoproterozoic	542–1,600	.7055	.7085	Undefined

Evolution of Pre-Tertiary Seawater Strontium Isotopes

The isotopic composition of seawater has evolved through time due to the balance of fluxes from continental (fluvial inputs), mantle (volcanic and hydrothermal activity at mid-ocean spreading centers), and continental shelf (diagenesis and dolomitization of marine carbonate) sources (Peterman and others, 1970; Burke and others, 1982; Faure,

1986; Peterman and Stuckless, 1992; Veizer and others, 1999, Faure and Mensing, 2005, p. 440). Determination of the seawater ^{87}Sr/^{86}Sr evolution curve is possible because Sr concentrations in biogenic carbonate are high (Sr readily substitutes for Ca, especially in the aragonite crystal structure) whereas radioactive ^{87}Rb [the parent isotope for ^{87}Sr with a half-life of 48.8 million years (m.y.)] is excluded. Therefore, seawater Sr is incorporated into the crystal structure of marine calcite or aragonite and remains unchanged with time in

rocks and carbonate fossils that have remained unmodified by secondary processes. Values of $^{87}Sr/^{86}Sr$ for Triassic through Cambrian brachiopods, belemnites, and conodonts and Neoproterozoic carbonate rocks from many locations around the world have been compiled to define the Paleozoic seawater $^{87}Sr/^{86}Sr$ evolution curve, shown in figure 3 along with bounding curves that represent probable uncertainties for mean seawater compositions at any one time period. Seawater $^{87}Sr/^{86}Sr$ values fluctuated from a high of around 0.7092 during the late Cambrian Period to a low of around 0.7070 in the late Permian Period with numerous fluctuations in between.

Post-depositional modification of $^{87}Sr/^{86}Sr$ can occur by several mechanisms including (1) accumulation of ^{87}Sr from the radioactive decay of small amounts of ^{87}Rb incorporated in the rock, especially in finely dispersed clay particles, (2) exchange of Sr with fluids during diagenesis or dolomitization, or (3) introduction of exotic strontium by hydrothermal fluids carrying radiogenic ^{87}Sr derived from basement sources (Peterman and others, 1994). These processes typically drive rock $^{87}Sr/^{86}Sr$ compositions toward higher (more radiogenic) values. Dolomites with low Sr concentrations may be particularly susceptible to subsequent introduction of exotic Sr.

Purpose and Scope

The purpose and scope of this report are to present chemical and $^{87}Sr/^{86}Sr$ data from cuttings and core samples of Paleozoic carbonate rocks from NTS boreholes (table 2) where ground-water data are available. Paleozoic rock samples from 20 boreholes in the Yucca Flat, Rainier Mesa, Frenchman Flat, and Mercury Valley were collected in 2005 and 2006 from zones within the LCA that produced water. In addition to these recently acquired data, chemical and isotopic data acquired from the same laboratory also are reported for rock samples obtained in the early and middle 1990s. These samples are from outcrops located outside the NTS and from two boreholes in the southwestern part of the NTS. These data are discussed in Peterman and others (1994), but were not published previously. Data in this report are presented in geospatial, tabular, and graphic forms, and are discussed in terms of the degree to which the compositions may have been modified by post-depositional chemical processes. However, no attempt is made to interpret these data with respect to water-rock interactions, reactive-transport mechanisms, or ground-water flow-path identification.
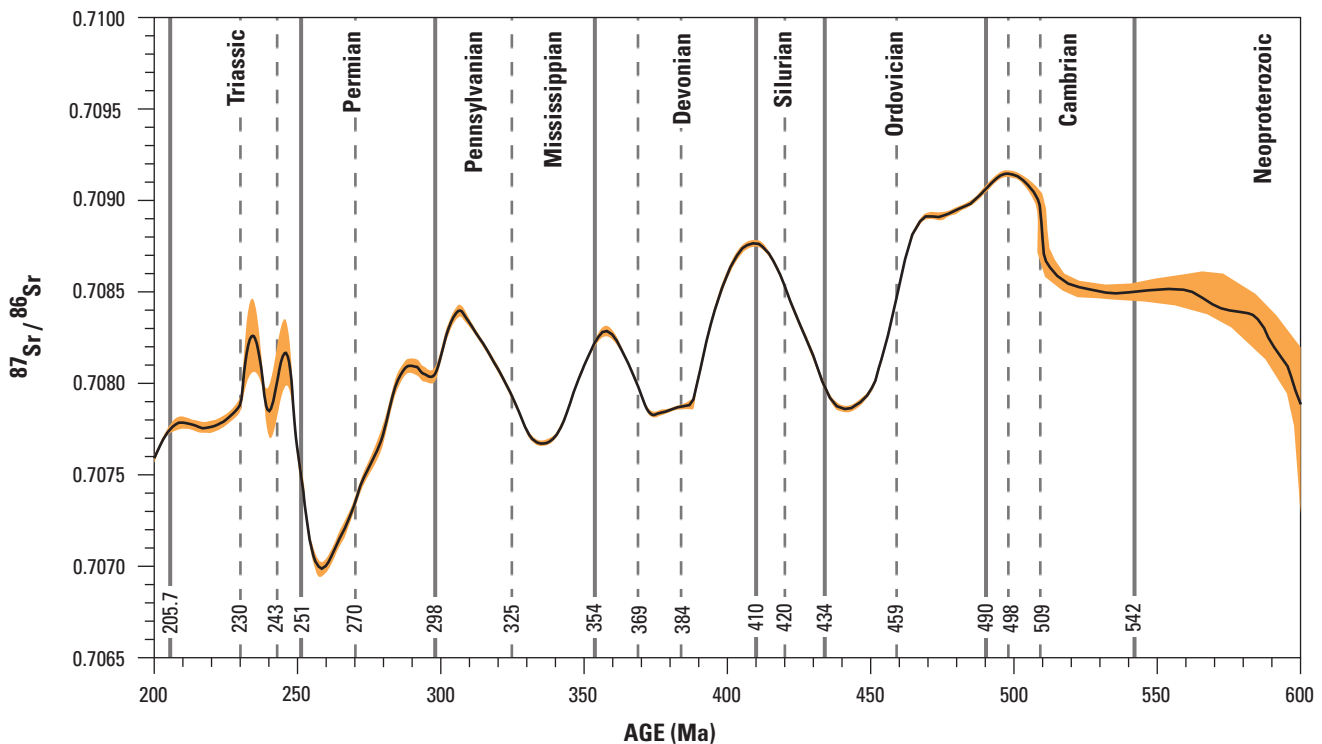
Figure 3.   Variation in strontium isotopic composition ($^{87}Sr/^{86}Sr$) of seawater during part of the Phanerozoic and Neoproterozoic based on analyses of unaltered brachiopods, belemnites, and conodonts from various locations worldwide. Dark curve represents the best-fit value for ages and $^{87}Sr/^{86}Sr$ values for data regressed by McArthur and others (2001) along with the 95-percent confidence level estimates (orange-shaded area). Solid vertical lines represent Period boundaries and dashed vertical lines represent Epoch boundaries based on the timescale of Young and Laurie (1996) as given in McArthur and others (2001), table 1.

Table 2.   Locations of boreholes from which core samples were obtained at the Nevada Test Site, Nye County, Nevada.

[Location of sampling sites are shown in figure 1*B*. Additional information on these and other boreholes associated with the Department of Energy weapons testing program at the Nevada Test Site is available at http://nevada.usgs.gov/mercury/core.html. **Abbreviations:** DOE, U.S. Department of Energy; USGS, U.S. Geological Survey**;** m, meter; UTM, Universal Transverse Mercator]

DOE borehole identification No.	Borehole identification No.	USGS site identification No.	UTM-Easting, zone 11 (m)	UTM-Northing, zone 11 (m)	Land surface elevation (m)	Date constructed	Borehole depth (m)
Army #1 Water Well	Army #1	363530116021401	586,120	4,049,800	961.1	07–15–62	595.3
ER–3–1	ER3–1	370116115561301	594,658	4,097,339	1,343.2	05–20–94	855.6
ER–5–3 #2	ER5–3 #2	365223115561801	594,624	4,081,120	1,016.3	03–20–01	1,732.2
ER–6–1 #2	ER6–1 #2	365901115593501	589,617	4,093,357	1,199.5	10–05–02	975.4
ER–6–2	ER6–2	365740116043501	582,236	4,090,745	1,289.7	07–21–94	1,045.5
ER–7–1	ER7–1	370424115594301	589,315	4,103,275	1,294.2	02–09–03	762.0
ER–12–1	ER12–1	371106116110401	572,412	4,115,493	1,773.1	11–24–92	1,093.6
ER–12–3	ER12–3	371142116125102	569,748	4,116,592	2,250.9	04–28–05	1,496.0
ER–12–4	ER12–4	371311116105902	572,473	4,119,346	2,097.9	06–01–05	1,132.3
ER–16–1	ER16–1	370031116121102	570,900	4,095,916	2,000.4	07–01–05	1,220.7
UE–1c	UE1c	370253116055201	580,223	4,100,394	1,282.2	02–11–64	573.0
UE–1h	UE1h	370005116040301	582,983	4,095,224	1,217.7	07–03–68	1,023.5
UE–2ce Water Well	UE2ce	370831116080701	576,804	4,110,773	1,452.2	01–23–77	502.9
UE–7nS	UE7nS	370556116000901	588,644	4,106,091	1,331.0	07–14–76	672.1
UE–10j	UE10j	371108116045301	581,527	4,115,645	1,394.1	02–24–93	796.4
UE–15d Water Well	UE15d	371230116021501	585,061	4,118,301	1,397.9	04–17–62	1,829.1
UE–16d Eleana Water Well	UE16d	370412116095101	574,301	4,102,761	1,427.7	03–03–81	914.4
UE–25 p #1	UE25p #1	364938116252102	551,509	4,075,663	1,113.9	05–24–83	1,805.0
UE–25 a #3	UE25a #3	365147116185301	561,079	4,079,703	1,385.6	10–10–78	771.1
USGS HTH #3	HTH #3	364830115512601	601,932	4,074,016	1,062.0	05–09–62	566.9
USGS Test Well C (WW-C)	TW–C	365508116003501	588,208	4,086,130	1,194.8	03–30–61	518.2
USGS Test Well D	TW–D	370418116044501	582,224	4,103,327	1,265.1	01–08–61	594.4

Analytical Methods

Core and cutting samples of Paleozoic rock core were obtained in 2006 from material archived at the U.S. Geological Survey (USGS) Core Library and Data Center in Mercury, Nevada. Intervals corresponding to water-producing zones were examined and samples were selected based on availability, representation of macroscopic features, and location in the stratigraphic section. Borehole intervals, sample types, stratigraphic units, and sample descriptions are given in table 3. Where only cuttings were available, samples with the largest fragment size were selected preferentially. In a few cases, special features were targeted, such as secondary calcite veins or altered breccia zones, to evaluate the differences between primary and secondary $^{87}Sr/^{86}Sr$ signatures; however, most samples were collected to evaluate unaltered, bulk-rock compositions. Stratigraphic units were assigned to samples using lithologic logs from borehole completion reports to DOE, which have been compiled recently by the U.S. Geological Survey (2006). Other sources include Maldonado and others, (1979) for borehole UE-25 a #3, and Carr and others, (1986) for borehole UE-25 p #1. These assignments were made by correlations with known stratigraphic sections or through biostratigraphic assignments, most commonly using conodonts (typically evaluated and reported as unpublished data by A. Harris, U.S. Geological Survey).

Table 3. Description of samples analyzed for strontium isotopic compositions from boreholes at the Nevada Test Site, Nye County, Nevada.

[**Stratigraphic units** are from lithology logs included in borehole completion reports to U.S. Department of Energy (see U.S. Geological Survey, 2006, for compilation of data and references, as well as Maldonado and others [1979], and Carr and others [1986]). Stratigraphic unit symbols are defined in table 1. Core and cutting samples were obtained in 2006 except for samples from boreholes UE–25 a #3 and UE–25 p #1, which were obtained in the early 1990s. Borehole depths are measured in feet below land surface. **Abbreviations:** DOE, Department of Energy; m, meter; mm, millimeter; >, greater than; <, less than; ±, plus or minus]

DOE borehole identification No.	Top depth (m)	Bottom depth (m)	Sample identification No.	Sample type	Stratigraphic unit symbol	Description
Army #1	261.8	261.8	Army 1(859)	Core	Cn-s	Mottled medium-to-dark grey, medium-grained limestone. Minor fractures filled with thin white secondary calcite. No alteration apparent.
	262.7	262.7	Army 1(862)	Core	Cn-s	Friable, altered limestone consisting of equant, medium-grained, dark grey calcite crystals with intergranular iron-stained (clayey?) material. Also, several fragments of other rock or vein material present as rounded clasts.
	299.3	302.4	Army 1(982)A	Core	Cn-h	Uniform, coarse-grained, medium-grey dolomite. Minor color mottling between light and medium grey.
	299.3	302.4	Army 1(982)B	Core	Cn-h	Thick (>15 mm) vein of sparry white-to-reddish tan calcite cutting grey dolomite. Sample isolates calcite vein from host rock.
	388.9	345.0	Army 1(1112)	Core	Cn-h	Highly broken and altered limestone. Original light grey, medium grained carbonate is highly fractured and altered to friable, brown clay-rich material.
	594.7	594.7	Army 1(1951)	Core fragments	Cb	Fragments of equigranular, coarse-grained, light-grey limestone with abundant fractures, some of which contain secondary cement and red-brown staining.
ER–3–1	694.9	698.0	ER3–1(2280)	Coarse cuttings	Cb	Medium-to-coarse grained, medium grey limestone.
	786.4	789.4	ER3–1(2580)	Cuttings	Cb	Massive fine-grained, light grey limestone.
ER–5–3#2	1,456.9	1,460.0	ER5–3 2(4780)	Cuttings	Dsv	Medium-to-coarse grained, pinkish grey limestone.
ER–6–1#2	661.4	664.5	ER6–1 2(2170)	Cuttings	Dsv	Coarse grained, white-to-light grey dolomite.
	801.6	804.7	ER6–1 2(2630)	Cuttings	Sl	Coarse grained, white-to-light grey dolomite.
	862.6	865.6	ER6–1 2(2830)	Cuttings	Sl	Coarse grained, white-to-light grey dolomite.
	911.3	914.4	ER6–1 2(2990)	Cuttings	Oes	Medium-to-coarse grained, grey dolomite.
ER–6–2	557.8	560.8	ER6–2(1830)	Cuttings	Cb	Medium-grained, grey limestone.
	648.9	648.9	ER6–2(2129)	Core	Cb	Uniform medium-grained, brownish grey dolomite with scattered thin fractures containing fine-grained white filling material.
	725.1	725.1	ER6–2(2379)	Core	Cb (mineralized fault)	Mottled medium-to-coarse grained, dark grey dolomite. Mottling is caused by irregular patches of coarser, lighter crystals surrounded by finer, darker crystals. Rock is cut by scattered thin, white-calcite-filled veins.
	796.4	796.4	ER6–2(2613)	Core	Dg	Medium-grained, medium grey limestone with numerous thin fractures filled with white secondary calcite. No evidence of staining or alteration.

Table 3.   Description of samples analyzed for strontium isotopic compositions from boreholes at the Nevada Test Site, Nye County, Nevada.—Continued

[**Stratigraphic units** are from lithology logs included in borehole completion reports to U.S. Department of Energy (see U.S. Geological Survey, 2006, for compilation of data and references, as well as Maldonado and others [1979], and Carr and others [1986]). Stratigraphic unit symbols are defined in <u>table 1</u>. Core and cutting samples were obtained in 2006 except for samples from boreholes UE–25 a #3 and UE–25 p #1, which were obtained in the early 1990s. Borehole depths are measured in feet below land surface. **Abbreviations:** DOE, Department of Energy; m, meter; mm, millimeter; >, greater than; <, less than; ±, plus or minus]

DOE borehole identification No.	Top depth (m)	Bottom depth (m)	Sample identification No.	Sample type	Stratigraphic unit symbol	Description
ER–6–2	829.5	829.5	ER6–2(2721.5)	Core	Dg (mineralized fault)	Mottled, fine-grained limestone consisting of light grey carbonate with extensive recrystallization and solution-breccia replacement textures. More-recent fractures commonly have light amounts of red staining.
ER–7–1	655.3	658.4	ER7–1(2150)	Coarse cuttings	Op	Very coarse-grained, medium grey limestone with patches or veins of finer grained carbonate that are either the same color as rock mass or lighter cream to reddish tan to brownish red.
	728.5	731.5	ER7–1(2390)	Coarse cuttings	Op	Cuttings of very coarse-grained, medium grey limestone with very uniform consistency. No veins or accessory phases observed, but many of the calcite crystals and fragment surfaces are mildly stained brownish red.
ER–12–1	524.3	527.3	ER12–1(1720)	Cuttings	Lower Dg or upper Dsi	Fine-to-medium grained carbonate including both medium grey and dark grey components. Both graphite and dispersed fine-grained pyrite are common, as are fragment surfaces coated with reddish-brown staining.
	1,018.0	1,021.1	ER12–1(3340)	Cuttings	Upper Dsv	Homogeneous sample of coarse-grained, white-to-light grey carbonate. Fragments are clean with no staining or other discoloration on surfaces.
ER–12–3	1,103.4	1,106.4	ER12–3(3620)	Cuttings	Mid to Late Ordovician	Uniform medium-grained, dark-grey dolomite with minor thin, white carbonate veins. Some veins are stained red.
	1,368.6	1,371.6	ER12–3(4490)	Cuttings	Mid Ordovician to Late Cambrian	Fine-to-coarse grained, light-to-dark grey limestone with minor color laminae in some fragments. Occassional thin, coarsely crystalline white carbonate veins. Minor iron staining.
	1,475.2	1,478.3	ER12–3(4840)	Cuttings	Mid Ordovician to Late Cambrian	Fine-to-coarse grained, medium-grey limestone with laminae in some fragments. Occasional thin white carbonate veins. Pyrite present on one fragment, but no noticable iron staining.
ER–12–4	786.4	789.4	ER12–4(2580)	Coarse cuttings	DSu	Cuttings dominated by medium- to coarse-grained, white-to-light grey dolomite. Small grains of an equant black mineral (oxidized pyrite?) are scattered throughout. Some surfaces have red staining.
	1,051.6	1,054.6	ER12–4(3450)	Coarse cuttings	Mid Ordovician to Late Cambrian	Cutting sample includes a range of dolomite fragments. Coarse-grained, white-greenish-grey fragments are dominant, but medium-grained, medium-to-dark grey fragments also are common.
	1,094.2	1,097.3	ER12–4(3590)	Cuttings	Mid Ordovician to Late Cambrian	Medium-to-coarse grained, medium-grey dolomite with abundant fine crystals of oxidized pyrite and coarse, white acicular mineral (tremolite?).

Table 3.   Description of samples analyzed for strontium isotopic compositions from boreholes at the Nevada Test Site, Nye County, Nevada.—Continued

[**Stratigraphic units** are from lithology logs included in borehole completion reports to U.S. Department of Energy (see U.S. Geological Survey, 2006, for compilation of data and references, as well as Maldonado and others [1979], and Carr and others [1986]). Stratigraphic unit symbols are defined in table 1. Core and cutting samples were obtained in 2006 except for samples from boreholes UE–25 a #3 and UE–25 p #1, which were obtained in the early 1990s. Borehole depths are measured in feet below land surface. **Abbreviations:** DOE, Department of Energy; m, meter; mm, millimeter; >, greater than; <, less than; ±, plus or minus]

DOE borehole identification No.	Top depth (m)	Bottom depth (m)	Sample identification No.	Sample type	Stratigraphic unit symbol	Description
ER–16–1	1,079.0	1,082.0	ER16–1(3540)	Cuttings	Dg	Cuttings are dominated by fine-grained, black carbonate with graphite-like sheen on surfaces. Other lithologies are present, but were excluded from sample.
	1,158.2	1,161.3	ER16–1(3800)	Cuttings	Dg	Medium-sized cuttings contain a heterogeneous suite of rock types, though most are carbonate. Lithologies range from coarse-grained, marble-like material to fine-grained, dark grey material similar to ER16–1(3540). Bulk material used for powder sample with no further picking.
HTH–3	563.9	566.9	HTH–3(1850)	Core fragments	Op	Fragments of equigranular, coarse-grained, medium-grey dolomite with abundant fractures, some of which contain micro-breccia and fine, white secondary cement ± brown staining.
TW–C	444.4	444.4	TW–C(1458)	Core	Dg	Medium-grained, grey limestone cut by numerous fractures filled with <1- to 5-mm-thick white secondary calcite veins. Minor red staining in some veins.
	446.6	446.6	TW–C(1463.5)	Core	Dg	Coarse-grained, mottled grey limestone with extensive secondary veining and recrystallization that yields solution-breccia textures in areas. Secondary calcite is white to brownish red.
TW–D	540.4	541.6	TW–D(1773)	Cuttings	Cn-d	Massive, fine-to-medium-grained, grey limestone. Coarse cuttings have spotty, clay-like coating on fragment surfaces.
UE–1c	545.6	548.6	UE1c(1790)	Coarse cuttings	Op	Coarse-grained, grey limestone. Several chips have fine-grained, brownish material that coat fracture surfaces or form thin veins.
	566.9	570.0	UE1c(1860)	Coarse cuttings	Op	Massive, fine-to-medium-grained, light pinkish to greenish brown limestone.
UE–1h	902.2	905.3	UE1h(2960)	Cuttings	Cn or Cb	Coarse grained, white-to-light grey dolomite.
UE–2ce	438.9	442.0	UE2ce(1440)	Cuttings	Cn or Cb	Coarse grained, white-to-light grey dolomite.
UE–7nS	625.5	625.5	UE7nS(2052.2)	Core	Op-av	Mottled limestone consisting of medium-to-coarse grained, light-brown limestone with irregular patches of fine-grained, brownish-red alteration product.
	667.5	667.5	UE7nS(2190)	Core	Op-av	Mottled coarse-grained limestone. Patches of coarse, light grey limestone are separated by lenses and veins of finer-grained, iron-stained material.
UE–10j	393.2	394.7	UE10j(1290)	Coarse cuttings	Cn-s	Massive, fine-to-medium-grained grey dolomite. Rock is highly fractured with very thin white, clay-like material commonly present in fractures.

Table 3.   Description of samples analyzed for strontium isotopic compositions from boreholes at the Nevada Test Site, Nye County, Nevada.—Continued

[**Stratigraphic units** are from lithology logs included in borehole completion reports to U.S. Department of Energy (see U.S. Geological Survey, 2006, for compilation of data and references, as well as Maldonado and others [1979], and Carr and others [1986]). Stratigraphic unit symbols are defined in <u>table 1</u>. Core and cutting samples were obtained in 2006 except for samples from boreholes UE–25 a #3 and UE–25 p #1, which were obtained in the early 1990s. Borehole depths are measured in feet below land surface. **Abbreviations:** DOE, Department of Energy; m, meter; mm, millimeter; >, greater than; <, less than]

DOE borehole identification No.	Top depth (m)	Bottom depth (m)	Sample identification No.	Sample type	Stratigraphic unit symbol	Description
UE–10j	567.8	567.8	UE10j(1863)	Core	Cn-h	Fine-grained, dark-grey dolomite with distinct 1-to-5-mm-thick bedding-plane laminations defined by thin, light brown stylolitic planes and thicker planes of white secondary calcite. Thin veins with white calcite also cut across bedding.
	625.1	625.1	UE10j(2051)	Core	Cn-d	Uniform, brownish-red, marly shale with conchoidal fracturing along shaley partings. Fine crystals are apparent under magnification. Some fracture surfaces have additional red staining.
	656.5	656.5	UE10j(2154)	Core	Cb-b	Massive coarse-grained, white-to-light grey dolomite. Minor fractures contain light brown staining.
UE–15d	1,816.6	1,817.8	UE15d(5960)	Core	Zj or Zn	Mostly medium-grained, grey dolomite with planar foliation defined by color streaks and grain elongation, but also patches of greenish white, coarse-grained dolomite breccia. Accessory pyrite present in both phases.
	1,827.0	1,827.0	UE15d(5994)	Core	Zj or Zn	Fine-grained, medium-grey dolomite with light-colored spots of coarser carbonate. Scattered fractures are filled with white secondary carbonate.
UE–16d	311.0	313.9	UE16d(1020)	Cuttings	PPt	Massive, fine-to-medium-grained, grey limestone.
	472.4	475.5	UE16d(1550)	Cuttings	MDe	Very coarse, white-to-light grey limestone concentrated from heterogeneous lithologies (including volcanic and fine-grained carbonates) in cuttings sample by extensive hand picking.
UE–25 a #3	43.3	43.4	UE25a3–142	Core	Mc or MDg	Dark grey, very-fine-grained shale/argillite.
	98.9	99.0	UE25a3–324	Core	Mc or MDg	Dark grey, very-fine-grained shale/argillite.
	150.4	150.5	UE25a3–493	Core	Mc or MDg	Dark grey, very-fine-grained shale/argillite.
	208.4	208.5	UE25a3–684	Core	Mc or MDg	Dark grey, very-fine-grained shale/argillite.
	263.0	263.1	UE25a3–863	Core	Mc or MDg	Dark grey, very-fine-grained shale/argillite.
	325.7	325.9	UE25a3–1069	Core	Mc or MDg	Dark grey, very-fine-grained shale/argillite.
	435.9	436.0	UE25a3–1430	Core	Mc or MDg	Light tannish-grey, thermally altered shale/argillite.
	525.0	525.1	UE25a3–1722	Core	Mc or MDg	Light grey, thermally altered shale/argillite.
	562.5	562.6	UE25a3–1846	Core	Mc or MDg	Light grey, thermally altered shale/argillite.
	637.8	637.9	UE25a3–2093	Core	Mc or MDg	Light grey, coarse-grained metasandstone.
	697.2	697.3	UE25a3–2287	Core	Mc or MDg	Light greenish-grey, calcareous argillite.
	741.1	741.2	UE25a3–2432	Core	Du	Dark orange-yellow, ferruginous clay seam.
	759.6	759.7	UE25a3–2492	Core	Du	White calcitic marble.
	766.4	766.5	UE25a3–2514	Core	Du	Light grey, laminated marble.
UE–25 p #1	1,277.9	1,278.0	HD–622	Core	DSlm	Light grey, massive, pelloidal dolomite.
	1,284.1	1,284.2	HD–621	Core	DSlm	Light grey, fine-grained, massive dolomite.
	1,798.3	1,798.4	UE25p 1–5900	Core	Sr	Dark grey, fine-grained dolomite with thin lamellae.

Samples from road cuts or outcrops were collected between 1989 and 1994 as part of a study to evaluate the usefulness of strontium isotopes as indicators of epithermal mineralization in areas surrounding Yucca Mountain, Nevada, the potential site for a geologic repository for high-level radioactive waste (Peterman and others, 1994). Samples of mineralized and unmineralized Paleozoic carbonate rocks were analyzed to represent geologic map units in several areas to the west, south, and east of the NTS (table 4; fig. 1). In addition, core samples from Paleozoic strata underlying the Tertiary volcanic rocks constituting Yucca Mountain (borehole UE-25 p #1) were included.

Samples of NTS core were split and representative fragments were selected for further processing. Samples of cuttings were examined under a binocular microscope and fragments of foreign material likely representing down-hole contamination by rock fragments from overlying lithologic units were removed. Final samples of cuttings and core fragments weighed between 3 and 50 grams (g). Outcrop samples were trimmed as much as possible in the field to remove weathering rinds or coatings of pedogenic carbonate and were subsampled further in the laboratory using a small diamond core drill (1.3-centimeter outside diameter). Resulting unweathered core samples ranged from 10 to 20 g. All samples were crushed and then pulverized to less than 0.075 millimeters using a steel shatterbox. All rock preparation and analyses were done by USGS Yucca Mountain Project Branch personnel in Denver, Colorado, between 1990 and 2006.

Analyses of the recently acquired NTS borehole samples were made on partial digestions (leachates) obtained by adding approximately 20 milliliters of 0.2 molar nitric acid to 0.1 g of rock powder. Acid solutions were allowed to react with rock powders in a 50°C incubator oven for 12 to 24 hours. Acid volumes were sufficient to maintain low pH in the final leachate solutions. Leachates then were analyzed for a selected suite of major and trace constituents (MgO, CaO, SiO_2, Al_2O_3, MnO, Rb, Sr, Th, and U) by inductively coupled plasma mass spectrometry (ICP-MS). Strontium was purified from the same leachates using Eichrom Sr-SPEC™ resin and $^{87}Sr/^{86}Sr$ isotopic compositions were measured using a Finnigan MAT 262™ multiple-collector thermal-ionization mass spectrometer operating in static mode. The instrument was calibrated using the USGS rock standard EN-1 (calcite from a modern *Tridacna* shell from Enewetok Lagoon in the western Pacific Ocean; Ludwig and others, 1988). To correct for instrument drift and eliminate small interlaboratory biases (Faure and Mensing, 2005, p. 78), measured $^{87}Sr/^{86}Sr$ values for samples in each magazine were normalized to the value obtained from the EN-1 standard measured in the same magazine and adjusted to an assigned value of 0.70920 for modern mean ocean water (Elderfield, 1986, p. 77). Replicate $^{87}Sr/^{86}Sr$ analyses of the uncorrected EN-1 standard varied by less than ±0.00005 (0.007 percent) at the 95-percent confidence level (2-sigma). Results for the National Institute of Standards and Technology strontium carbonate standard, SRM 987,

(accepted $^{87}Sr/^{86}Sr$ value of 0.71025; Faure and Mensing, 2005, p. 79) analyzed between 1997 and 2006 yielded a weighted average $^{87}Sr/^{86}Sr$ value of 0.710270 ±0.000011 (95-percent confidence limit) indicating that estimates of accuracy and precision are similar. Sr contributions from the chemical procedure (blank) were approximately 2×10^{-9} g, which are 5–7 orders of magnitude lower than the total amount of Sr contributed from the samples.

Rock powders from outcrop samples were analyzed before ICP-MS capabilities became available. Instead, selected elements (Rb, Sr, Y, Zr, Nb, Ba, La, and Ce) were analyzed by energy-dispersive XRF (X-ray fluorescence) spectroscopy on bulk rock powders. Results for the rock-forming constituents MgO and CaO are not available. $^{87}Sr/^{86}Sr$ was analyzed in the carbonate fraction by dissolving subgram powdered aliquots in 1 molar hydrochloric acid followed by purification of Sr using cation exchange resins. $^{87}Sr/^{86}Sr$ values were measured using either the instrument described in the previous paragraph, or on one of two single collector instruments (National Bureau of Standards instrument or VG Isomass 54E) operating in peak-hopping mode. The measurements were treated identically to those described above using results of EN-1 to normalize unknown $^{87}Sr/^{86}Sr$ values. Samples of drill core obtained in the early 1990's from UE-25 p #1 (fig. 1B) were processed in the same manner as outcrop samples. Samples of Gap Wash Formation siliciclastic rocks (Eleana Formation equivalent; Trexler and others, 2003) from UE-25 a #3 (fig. 1B) as well as two of the outcrop samples (HD-1107 and HD-1114 with respective Map No. 4 and 5 in table 4) were digested using hydrofluoric and sulfuric acids prior to Sr purification.

To emphasize small but significant variations in $^{87}Sr/^{86}Sr$, data also are reported as per mil (‰) deviations from modern seawater ($^{87}Sr/^{86}Sr = 0.70920$) using the equation

$$\delta^{87}Sr = \left(\frac{^{87}Sr/^{86}Sr_{unknown}}{0.70920} - 1 \right) \times 1{,}000. \quad (1)$$

Analytical uncertainties in $\delta^{87}Sr$ values are typically less than ±0.07 per mil at the 95-percent confidence level. Although modern seawater provides a useful reference point for comparative purposes, it is desirable to know whether present-day $^{87}Sr/^{86}Sr$ compositions of the marine carbonate rocks have been modified from seawater $^{87}Sr/^{86}Sr$ compositions that were present at the time of deposition. Therefore, $\delta^{87}Sr_t$ values are computed using stratigraphic age assignments and paleoseawater $^{87}Sr/^{86}Sr$ compositions using the equation,

$$\delta^{87}Sr_t = \left(\frac{^{87}Sr/^{86}Sr_{unknown}}{^{87}Sr/^{86}Sr_{paleoseawater}} - 1 \right) \times 1{,}000, \quad (2)$$

where $^{87}Sr/^{86}Sr_{paleoseawater}$ is derived from figure 3 and the stratigraphic ages listed in table 1. Explicit uncertainties for $\delta^{87}Sr_t$ are not given in this report because of the difficulty in defining uncertainties to the age assignments. However, they are expected to be as much as an order of magnitude larger than those for $\delta^{87}Sr$.

Table 4.   Locations, stratigraphic unit designations, and descriptions of outcrop samples analyzed for strontium isotopic compositions from the Nevada Test Site vicinity, Clark, Lincoln, and Nye Counties, Nevada, and Inyo County, California.

[Map numbers are used to locate sites in figure 1. **Stratigraphic units** are from geologic maps listed in the text. **Stratigraphic unit** symbols are defined in table 1. **Abbreviations:** cm, centimeter; m, meter; UTM, Universal Transverse Mercator]

Map No.	Sample identification No.	Area	Locality	UTM Easting (m)	UTM Northing (m)	Strati-graphic unit	Description
1	HD–1106	Funeral Mountains	Chloride City	510,520	4,061,767	ZYb	Calcitic marble.
2	HD–1111	Funeral Mountains	Chloride City	510,222	4,061,921	ZYc	Coarse-grained, thinly bedded marble.
3	HD–1112	Funeral Mountains	Chloride City	510,222	4,061,921	ZYc	Coarse-grained, thinly bedded marble.
4	HD–1107	Funeral Mountains	Chloride City	510,869	4,060,843	ZYb	Coarse-grained, thinly laminated dolomite with graphite layers.
5	HD–1114	Funeral Mountains	Chloride City	510,271	4,062,537	ZYc	Light grey, fine-grained, saccharoidal marble.
6	HD–1105	Funeral Mountains	East of Chloride City	511,883	4,063,433	Zs-c	Purple grey dolomite; weathers to reddish brown.
7	HD–1151	Bare Mountain	Beatty	521,387	4,081,908	CZw	Buff, thinly banded limestone interbedded with quartzite beds.
8	3C–1	Bare Mountain	Black Marble Hill	533,950	4,066,327	Cb	Not available.
9	HD–212	Bare Mountain	Black Marble Hill	533,424	4,067,650	Cb	Dolomite.
10	HD–214	Bare Mountain	Black Marble Hill	533,424	4,067,650	Cb	Intact dolomite.
11	HD–216	Bare Mountain	Black Marble Hill	533,424	4,067,650	Cb	Intact dolomite.
12	HD–218	Bare Mountain	Black Marble Hill	533,424	4,067,650	Cb	Intact dolomite.
13	HD–219	Bare Mountain	Black Marble Hill	533,424	4,067,650	Cb	Intact dolomite.
14	HD–220	Bare Mountain	Black Marble Hill	533,424	4,067,650	Cb	Bleached/tan dolomite.
15	HD–221	Bare Mountain	Black Marble Hill	533,424	4,067,650	Cb	Intact dolomite.
16	HD–1154	Bare Mountain	Carrara Canyon	528,539	4,074,996	CZw-u	Chocolate-brown, well-bedded limestone.
17	HD–1155	Bare Mountain	Carrara Canyon	528,613	4,075,089	CZw	Chocolate-brown, well-bedded limestone.
18	HD–538	Bare Mountain	Carrara Canyon	529,207	4,075,399	Cb-p	Very light grey, fine-to-medium grained calcitic marble.
19	HD–539	Bare Mountain	Carrara Canyon	529,330	4,075,615	Cb-p	Medium-to-dark grey fine-grained mottled dolomite with laminated texture and intervals containing partings of light brown silty dolomite.
20	HD–540	Bare Mountain	Carrara Canyon	529,157	4,075,584	Cb-p	Mottled dark and light grey, fine-grained dolomite.
21	HD–541	Bare Mountain	Carrara Canyon	528,539	4,074,996	CZw-u	Light brown, medium grained calcitic marble with minor grains of quartz sand.
22	HD–513	Bare Mountain	Chuckwalla Canyon	531,820	4,078,706	Oes	Medium grey, recrystallized dolomite with laminae of secondary chert.
23	HD–515	Bare Mountain	Chuckwalla Canyon	531,845	4,078,860	Oes	Medium light grey, fine-grained recrystallized dolomite.
24	HD–516A	Bare Mountain	Chuckwalla Canyon	531,844	4,078,891	Sr	Medium dark grey, laminated, recrystallized dolomite.
25	HD–517	Bare Mountain	Chuckwalla Canyon	531,795	4,078,983	Sr	Medium grey, laminated, fine-grained recrystallized limestone.
26	HD–518	Bare Mountain	Chuckwalla Canyon	531,794	4,079,106	Sr	Medium grey, fine-grained, crystallized dolomite with sparse lenses of chert and calcified macrofossils.

Table 4.   Locations, stratigraphic unit designations, and descriptions of outcrop samples analyzed for strontium isotopic compositions from the Nevada Test Site vicinity, Clark, Lincoln, and Nye Counties, Nevada, and Inyo County, California.—Continued

[Map numbers are used to locate sites in figure 1. **Stratigraphic units** are from geologic maps listed in the text. **Stratigraphic unit** symbols are defined in table 1. **Abbreviations:** cm, centimeter; m, meter; UTM, Universal Transverse Mercator]

Map No.	Sample identification No.	Area	Locality	UTM Easting (m)	UTM Northing (m)	Strati-graphic unit	Description
27	HD–519	Bare Mountain	Chuckwalla Canyon	531,769	4,079,137	DSlm	Very light grey, fine-grained recrystallized dolomite.
28	HD–520	Bare Mountain	Chuckwalla Canyon	531,944	4,078,644	DSlm	Light grey, fine-grained dolomite with white dolomitic mottling and crinoid debris.
29	HD–533	Bare Mountain	Diamond Queen Mine	532,270	4,077,721	Op-av	Mottled light-to-medium grey, fine-grained limestone with massive texture and veins of pinkish grey carbonate.
30	HD–534	Bare Mountain	Diamond Queen Mine	532,271	4,077,536	Op-g	Medium light grey thin-bedded limestone with irregular light-brown silty partings.
31	HD–535	Bare Mountain	Diamond Queen Mine	532,372	4,076,951	Cn-s	Medium light grey, fine-to-medium grained recrystallized dolomite with massive texture.
32	HD–1415	Bare Mountain	Fluorspar Canyon	523,463	4,083,239	Cb-p	Unaltered carbonate.
33	HD–1416	Bare Mountain	Fluorspar Canyon	523,488	4,083,177	Cb-p	Unaltered carbonate.
34	HD–1417	Bare Mountain	Fluorspar Canyon	522,993	4,083,084	CZw-l	Lower member, Unit D.
35	HD–1418	Bare Mountain	Fluorspar Canyon	522,919	4,083,114	CZw-l	Lower member, Unit D.
36	HD–1419	Bare Mountain	Fluorspar Canyon	522,968	4,083,145	Cb-p	Unaltered carbonate.
37	HD–1420	Bare Mountain	Fluorspar Canyon	522,893	4,083,237	Cb-p	Unaltered carbonate.
38	HD–1421	Bare Mountain	Fluorspar Canyon	522,745	4,083,114	CZw-l	Lower member, Unit D; Sandy brown limey quartzite.
39	HD–527	Bare Mountain	Fluorspar Canyon	528,094	4,082,390	Df	Light grey, fine-grained recrystallized dolomite. Brecciated with local cementation of thin silica veinlets.
40	HD–528	Bare Mountain	Fluorspar Canyon	527,798	4,081,927	Df	Light-to-dark grey, fine-grained dolomite laced with boxwork of white dolomite veinlets.
41	HD–529	Bare Mountain	Fluorspar Canyon	526,562	4,081,492	Cb-b	Very light grey, fine- to medium-grained calcitic marble.
42	HD–530	Bare Mountain	Fluorspar Canyon	526,562	4,081,584	Cb-b	Medium light grey, fine-grained dolomitic marble.
43	HD–531	Bare Mountain	Fluorspar Canyon	526,636	4,081,677	Cn-h	Medium-to-dark grey, fine-grained calcitic marble with thin layers of dolomitic marble and olive-grey chert.
44	HD–542	Bare Mountain	Fluorspar Canyon	523,018	4,082,868	CZw-l	Pale orange, fine-grained dolomitic marble.
45	HD–543	Bare Mountain	Fluorspar Canyon	523,883	4,083,271	Cb-p	Light grey, fine-grained dolomitic marble.
46	HD–1152b	Bare Mountain	Gold Ace Mine	526,504	4,076,346	Zs-d	Altered limestone with solution boxworks.
47	HD–1153	Bare Mountain	Gold Ace Mine	526,653	4,076,161	Zs-d	Buff (weathered) to grey (fresh) siliceous limestone.
48	HD–1142	Bare Mountain	Secret Pass	529,582	4,081,471	Op-g	Grey, thinly bedded limestone.
49	HD–1144	Bare Mountain	Secret Pass	529,359	4,081,439	Df	Medium grey, fairly massive, highly fractured limestone.

Table 4.   Locations, stratigraphic unit designations, and descriptions of outcrop samples analyzed for strontium isotopic compositions from the Nevada Test Site vicinity, Clark, Lincoln, and Nye Counties, Nevada, and Inyo County, California.—Continued

[Map numbers are used to locate sites in figure 1. **Stratigraphic units** are from geologic maps listed in the text. **Stratigraphic unit** symbols are defined in table 1. **Abbreviations:** cm, centimeter; m, meter; UTM, Universal Transverse Mercator]

Map No.	Sample identification No.	Area	Locality	UTM Easting (m)	UTM Northing (m)	Strati-graphic unit	Description
50	HD–1400	Bare Mountain	Sterling Mine	532,006	4,075,440	Cb-b	Unaltered carbonate.
51	HD–1401	Bare Mountain	Sterling Mine	532,006	4,075,440	Cb-b	Unaltered carbonate.
52	HD–1402	Bare Mountain	Sterling Mine	532,006	4,075,440	Cb-b	Unaltered carbonate.
53	HD–641	Bare Mountain	Sterling Mine	532,057	4,075,132	Cb-b	Country rock adjacent to "red ore".
54	HD–537	Bare Mountain	Steves Pass	533,101	4,067,802	Zs-d	Light brown, fine-to-medium grained recyrstallized dolomite.
55	HD–1146	Bare Mountain	Tarantula Canyon	531,147	4,080,121	MDe	Thin-bedded limestone consisting of rusty brown layers that are more resistant to weathering than medium grey limestone.
56	HD–1147a	Bare Mountain	Tarantula Canyon	532,039	4,079,908	Dtc	Massive medium grey limestone with reddened zones, especially along fractures and bedding planes.
57	HD–1147b	Bare Mountain	Tarantula Canyon	532,039	4,079,908	Dtc	Massive medium grey limestone with reddened zones, especially along fractures and bedding planes.
58	HD–522	Bare Mountain	Tarantula Canyon	532,806	4,080,034	Dtc	Very light-grey, fine-grained dolomite.
59	HD–523	Bare Mountain	Tarantula Canyon	532,681	4,080,188	Dtc	Medium-to-dark grey, fine-grained limestone with sparse chert nodules and minor calcite veins.
60	HD–526	Bare Mountain	Tarantula Canyon	530,106	4,080,425	Cc-m	Medium grey, fine-grained limestone mottled with light-olive-grey silty dolomite and cut by thin crystalline calcite veins.
61	HD–1138	Bare Mountain	Telluride Mine	531,008	4,084,064	Op-av	Medium grey, thinly bedded limestone with numerous secondary calcite vieins.
62	HD–1139	Bare Mountain	Telluride Mine	530,935	4,083,971	DSlm	Massive to brecciated dolomite and limestone.
63	HD–1141	Bare Mountain	Telluride Mine	531,234	4,083,387	Op-av	Thinly bedded limestone with 2- to 6-cm-thick layers of alternating medium grey and greyish tan beds.
64	HD–1150b	Bare Mountain	Tungsten Canyon	530,850	4,073,217	CZw	Orange-weathering carbonate.
65	HD–546	Striped Hills	Outlier on west side	556,896	4,057,913	Dn	Light-to-medium grey, fine-grained massive dolomite with mottling and brecciation. Light red ion oxide coatings on fracture surfaces.
66	HD–548	Striped Hills	West side	559,200	4,058,576	Op-av	Medium- to dark-grey, rusty-weathering, silty limestone.
67	HD–549	Striped Hills	West side	559,152	4,058,390	Op-g	Medium- to dark-grey limestone containing thin rusty-weathered lenses and fractures.
68	HD–550	Striped Hills	West side	559,177	4,058,298	Op-g	Medium- to dark-grey, very fine-grained limestone containing tan to pinkish grey silty laminae.

Table 4.   Locations, stratigraphic unit designations, and descriptions of outcrop samples analyzed for strontium isotopic compositions from the Nevada Test Site vicinity, Clark, Lincoln, and Nye Counties, Nevada, and Inyo County, California.—Continued

[Map numbers are used to locate sites in figure 1. **Stratigraphic units** are from geologic maps listed in the text. **Stratigraphic unit** symbols are defined in table 1. **Abbreviations:** cm, centimeter; m, meter; UTM, Universal Transverse Mercator]

Map No.	Sample identification No.	Area	Locality	UTM Easting (m)	UTM Northing (m)	Strati- graphic unit	Description
69	HD–551A	Striped Hills	West side	558,739	4,057,093	Op-g	Medium-grey, medium-grained dolomite with red staining on microfractures.
70	HD–553	Striped Hills	West side	558,959	4,057,557	Cn-h	Medium- to dark-grey, very fine-grained limestone containing fractures with red-stained coatings on fractures.
71	HD–554	Striped Hills	West side	558,835	4,057,464	Cb-b	Light- and dark-grey, medium grained limestone with reddish iron oxide coatings on fracture surfaces.
72	HD–555	Striped Hills	West side	558,168	4,057,028	Cb-b	Medium-to-dark grey, very fine-grained limestone containing fractures with red-stained coatings on fractures.
73	HD–556	Striped Hills	West side	558,145	4,056,781	Cb-b	Light-to-medium grey, fine- to medium-grained limestone with thin fractures of secondary calcite.
74	HD–557	Striped Hills	West side	558,099	4,056,288	Cb-p	Light-to-medium grey, medium-grained limestone with mottling and buff to light grey coatings on fracture surfaces.
75	HD–558	Striped Hills	West side	558,025	4,056,164	Cb-p	Mottled medium grey, fine-grained laminated limestone with patches of reddish iron oxide and white crystalline calcite.
76	HD–1422–1	Specter Range	Rock Valley Wash	562,215	4,053,605	Cb-b	Altered carbonate.
77	HD–1422–2	Specter Range	Rock Valley Wash	562,215	4,053,605	Cb-b	Altered carbonate.
78	HD–1423	Specter Range	Rock Valley Wash	562,191	4,053,512	Cb-b	Unaltered carbonate.
79	HD–1426	Specter Range	Central	569,490	4,053,907	CZw	Rusty-weathering dolomitic quartzite.
80	HD–1427	Specter Range	Central	571,247	4,057,681	Cb-b	Upper Bonanza King Formation with possible mineralization and thin rusty-colored veins throughout.
81	HD–1428	Specter Range	Central	570,884	4,056,569	Cb-b	Light grey massive carbonate.
82	HD–1429	Specter Range	Central	569,881	4,054,743	Cb-p	Lower Bonanza King carbonate.
83	HD–1432	Specter Range	Central	570,824	4,048,741	DSu	Medium grey, porous carbonate.
84	HD–1434	Specter Range	Point of Rocks Area	579,083	4,050,601	Dsv	Brecciated carbonate.
85	HD–1435	Specter Range	Point of Rocks Area	580,589	4,049,012	Cb	Massive white marble.
86	HD–1436	Specter Range	Point of Rocks Area	582,172	4,047,178	Cb-b	Unaltered carbonate.
87	HD–110–1	Devils Hole Hills	Above Devils Hole	563,572	4,031,182	Cb-b	Dark grey limestone.
88	HD–471B	Devils Hole Hills	Above Devils Hole	563,448	4,031,120	Cb-b	Unaltered carbonate.
89	GDR–8	Spring Mountains	Cold Creek Spring	613,012	4,027,188	Cu	Unaltered carbonate.
90	HD–229	Spring Mountains	Lower Lee Canyon	634,380	4,031,346	PMbl	Well bedded limestone with alternating medium grey and more weather-resistant medium tan layers.
91	HD–230	Spring Mountains	Lower Lee Canyon	628,327	4,029,589	PMbl	Thick-bedded-to-massive tan limestone.

Table 4.   Locations, stratigraphic unit designations, and descriptions of outcrop samples analyzed for strontium isotopic compositions from the Nevada Test Site vicinity, Clark, Lincoln, and Nye Counties, Nevada, and Inyo County, California.—Continued

[Map numbers are used to locate sites in figure 1. **Stratigraphic units** are from geologic maps listed in the text. **Stratigraphic unit** symbols are defined in table 1. **Abbreviations:** cm, centimeter; m, meter; UTM, Universal Transverse Mercator]

Map No.	Sample identification No.	Area	Locality	UTM Easting (m)	UTM Northing (m)	Strati-graphic unit	Description
92	HD–231	Spring Mountains	Lower Lee Canyon	627,318	4,028,773	Mm	Medium grey, massive limestone.
93	HD–232	Spring Mountains	Upper Lee Canyon	620,905	4,022,271	Cb-b	Highly fractured, medium grey limestone with some silty layers.
94	HD–233	Spring Mountains	Upper Lee Canyon	619,928	4,020,839	Cb-b	White -to-light buff, coarse-grained limestone.
95	HD–235	Spring Mountains	Upper Lee Canyon	618,762	4,018,574	Cn	White-to-light buff, coarse-grained, thinly laminated limestone.
96	HD–236	Spring Mountains	Upper Lee Canyon	622,300	4,022,414	Op	Medium grey, poorly bedded limestone with high degree of fracturing.
97	HD–238	Spring Mountains	Kyle Canyon	637,123	4,015,392	PMb	Light grey, thick bedded-to-massive limestone that weathers to light buff.
98	HD–1000	Sheep Range	Black Hills	649,365	4,049,285	Dg	Light-grey, thickly bedded limestone with tension-gash veins common.
99	HD–999	Sheep Range	Black Hills	646,898	4,048,163	Cn-s	Black, fine-grained laminated dolomite.
100	HD–995	Pintwater Range	Southern end	625,873	4,049,217	Oes	Dark-black, fine-grained dolomite with local cherty layers.
101	HD–996	Pintwater Range	Southern end	626,955	4,051,698	Op-av	Dolomitized limestone with layers of nodular chert.
102	HD–997	Pintwater Range	Southern end	628,655	4,054,344	Oes	Black, fine-grained laminated dolomite, locally brecciated.
103	HD–998	Pintwater Range	Southern end	627,652	4,054,945	Op-av	Medium grey limestone with abundant bioturbation and macrofossils.
104	HD–1001	Pintwater Range	Northeast side	631,216	4,089,675	Op-av	Brownish, locally dolomitized limestone
105	HD–1006	Pintwater Range	Northwest side	621,872	4,094,313	Op-av	Grey limestone.
106	HD–990	Indian Springs Valley	Nellis Air Force Base	619,875	4,051,504	Op-av	Dark grey limestone.
107	HD–1002	Indian Springs Valley	Central	623,337	4,069,985	Oes	Medium grey to tan, coarsely saccharoidal dolomite.
108	HD–991	Indian Springs Valley	West side	614,367	4,054,604	Oes	Black, fine-grained dolomite.
109	HD–993	Spotted Range	Eastern side	610,588	4,058,715	Dsi	Grey, medium-grained dolomite.
110	HD–994	Spotted Range	Central	607,444	4,061,911	Mj	Black, coarse-grained limestone with abundant crinoid debris.
111	HD–1004	Spotted Range	Northeast side	618,367	4,070,685	Op-av	Grey limestone with local silty laminations.
112	HD–1003	Spotted Range	Northeast side	620,405	4,075,645	Dg	Dark grey, fine-grained, massive limestone.
113	HD–1007	Yucca Flat	North end Eleana Range	574,337	4,115,797	Op-g	Medium grey, fossiliferous, thin-bedded limestone.
114	HD–1008	Yucca Flat	North end Eleana Range	572,367	4,115,472	Dsv	Dark grey, medium-grained, thick-bedded dolomite.

Major and Trace Element Chemistry

Most of the borehole samples (34 of 48) were readily soluble losing 90.9 to 100 percent of their original sample weight during the 0.2 molar nitric acid treatment (table 5). The remaining 14 samples lost between 4.1 and 86.8 percent of the original sample weight. The greater amounts of residue in these samples are assumed to consist mostly of silicate material. Most samples were readily identifiable as limestone or dolomite, based on their CaO and MgO contents (diamonds on fig. 4). Assuming that all of the dissolved CaO and MgO is derived from the carbonate fraction, calcite ($CaCO_3$) mole percentages vary from 93.2 to 99.6 percent in limestone

samples and 48.0 to 53.6 percent in most dolomite samples. A small number of samples have intermediate MgO contents, resulting in calcite mole percentages between 55.6 and 74.2 percent. These values exceed the amount of calcite that can substitute into the dolomite crystal structure (Gaines and others, 1997, p. 450). The resulting linear trend between calcite and dolomite stoichiometric end members indicates that these samples represent mixtures of the two phases. Samples with intermediate compositions include core, cuttings, and a discrete sample of sparry vein carbonate [Army#1(982) B]. This observation indicates that excess $CaCO_3$ contents are intrinsic to some dolomite samples and are not the result of down-hole mixing of cutting fragments.
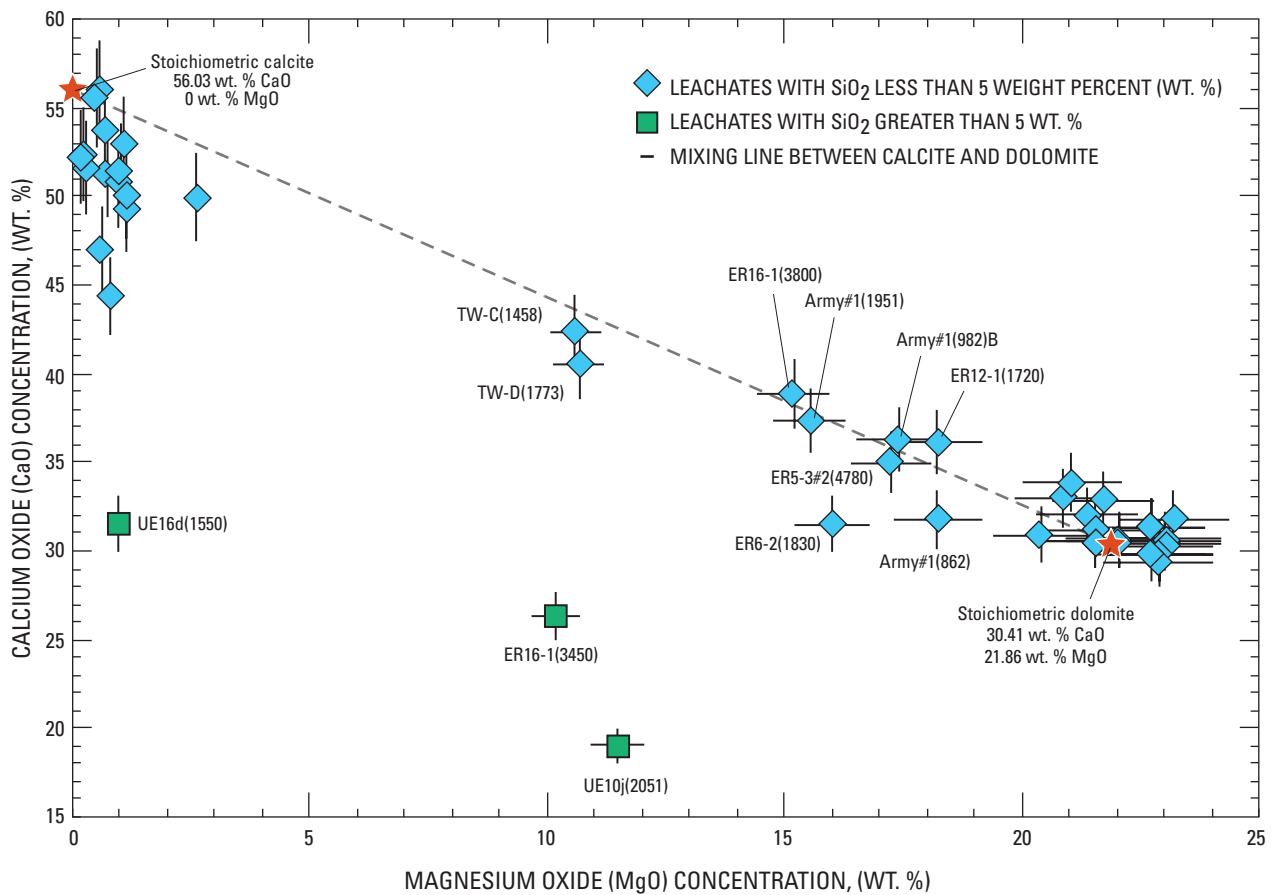

Figure 4.   Relation between magnesium oxide (MgO) and calcium oxide (CaO) concentrations in acid leachates of borehole samples, Nevada Test Site, Nye County, Nevada. Sample descriptions and data are from tables 3 and 5. Error bars represent 2-sigma analytical uncertainty and are shown as 5 percent of the reported concentration value.

Table 5. Oxide and elemental concentrations and strontium isotopic compositions ($^{87}Sr/^{86}Sr$) of nitric-acid leachates of core samples from boreholes at the Nevada Test Site, Nye County, Nevada.

[Results are for samples collected and analyzed in 2006. Oxide concentrations are given in weight percentages, and elemental concentrations are given in micrograms per gram. The less than (<) symbol is used to indicate concentrations that are below minimum reporting limits and incorporate the measured dilution factors for each sample; the greater than (>) symbol is used to indicate concentrations that are above the range of standards used to define the calibration curve. Uncertainties for strontium isotopic compositions ($^{87}Sr/^{86}Sr$) are dominated by external errors for replicate analyses of the Sr isotope standard EN-1, therefore, a blanket $^{87}Sr/^{86}Sr$ uncertainty of 0.00005 is reported. Strontium isotopic compositions also are given in delta notation ($\delta^{87}Sr = [(^{87}Sr/^{86}Sr_{sample}/^{87}Sr/^{86}Sr_{msw})-1]$ $\times 1{,}000$ and $\delta^{87}Sr_t = [(^{87}Sr/^{86}Sr_{sample}/^{87}Sr/^{86}Sr_{psw})-1]\times 1{,}000$, where $^{87}Sr/^{86}Sr_{msw}$ is the value for modern seawater and $^{87}Sr/^{86}Sr_{psw}$ is the value for paleoseawater at the time of deposition). **Abbreviations:** MgO, magnesium oxide; CaO, calcium oxide; $CaCO_3$, calcium carbonate (calcite); SiO_2, silicon dioxide; Al_2O_3, aluminum oxide; MnO, manganese oxide; Rb, rubidium; Sr, strontium; Th, thorium; U, uranium; ‰, permil]

Sample identification No.	Percent sample dissolved	MgO	CaO	Mole percent $CaCO_3$	SiO_2	Al_2O_3	MnO	Rb	Sr	Th	U	$^{87}Sr/^{86}Sr$ (±0.00005 2σ)	$\delta^{87}Sr$, ‰ (±0.07 2σ)	$\delta^{87}Sr_t$, ‰	Seawater $^{87}Sr/^{86}Sr_{psw}$ used
Army 1(859)	98.8	22.7	31.3	49.8	0.21	0.02	0.016	<0.79	30.4	<0.23	<0.23	0.70856	-0.90	-0.62	0.7090
Army 1(862)	69.2	18.2	31.8	55.6	1.69	1.10	.017	6.73	69.6	4.02	.55	.71132	2.99	3.27	.7090
Army 1(982)A	97.9	22.9	30.2	48.7	.22	.01	.026	< .87	30.7	< .26	< .26	.71027	1.51	1.65	.7091
Army 1(982)B	98.5	17.4	36.2	59.9	.23	.02	.018	< .88	37.9	< .26	< .26	.71023	1.45	1.59	.7091
Army 1(1112)	33.5	.81	44.4	97.5	3.14	1.85	.260	11.3	364	20	< .88	.71098	2.50	2.64	.7091
Army 1(1951)	100.0	15.5	37.4	63.3	.19	.01	.005	< .75	107	< .23	.28	.70935	.22	.22	.7092
ER3–1(2280)	98.8	2.6	50.0	93.2	< .20	.02	.027	< .94	543	< .28	< .28	.70958	.54	.54	.7092
ER3–1(2580)	99.7	1.1	49.3	96.9	< .22	.01	.004	<1.04	243	< .31	< .31	.70935	.20	.20	.7092
ER5–3 2(4780)	99.4	17.2	35.0	59.3	< .20	.03	.014	< .93	79.4	< .27	< .27	.71084	2.32	3.17	.7086
ER6–1 2(2170)	99.1	23.0	30.5	48.8	< .20	.02	.011	< .95	60.2	< .28	.75	.70809	-1.57	- .02	.7082
ER6–1 2(2630)	100.0	23.0	30.6	48.9	< .17	.01	.015	< .80	53.2	< .24	.54	.70816	-1.47	- .06	.7082
ER6–1 2(2830)	100.0	22.9	29.8	48.4	< .19	.01	.012	< .89	44.5	< .26	.41	.70825	-1.33	.08	.7082
ER6–1 2(2990)	95.6	23.0	30.4	48.6	.27	.06	.018	< .90	77.1	< .28	1.53	.70851	- .98	.01	.7085
ER6–2(1830)	79.3	16.0	31.5	58.6	1.55	> .97	.038	7.28	140	2.29	< .30	.71227	4.33	4.47	.7091
ER6–2(2129)	96.9	21.7	32.9	52.1	.54	< .08	.026	.88	70.5	< .26	< .26	.70854	- .92	- .50	.7089
ER6–2(2379)	97.7	21.1	33.9	53.6	.47	< .08	.014	< .84	47.0	< .26	.59	.71042	1.73	2.15	.7089
ER6–2(2613)	98.0	.71	51.4	98.1	.39	.01	.005	<1.02	103	< .29	.66	.70897	- .33	.94	.7083
ER6–2(2721.5)	98.5	.95	50.8	97.5	.36	< .08	.006	< .80	97.6	< .25	.33	.71103	2.58	3.86	.7083
ER7–1(2150)	90.9	.59	56.0	98.5	< .24	.03	.007	<1.12	425	< .34	.39	.70889	- .44	- .01	.7089
ER7–1(2390)	96.9	.49	55.5	98.8	< .18	.02	.004	< .86	452	.38	.36	.70884	- .50	- .08	.7089
ER12–1(1720)	51.2	18.2	36.1	58.7	.68	.45	.053	4.78	297	1.94	2.14	.71406	6.86	8.70	.7079
ER12–1(3340)	97.5	23.2	31.8	49.6	< .21	.01	.016	< .96	40.1	< .29	1.12	.71013	1.32	3.15	.7079
ER12–3(3620)	97.4	22.7	31.3	49.8	< .18	< .08	.012	< .84	105	< .25	.30	.70908	- .16	.26	.7089
ER12–3(4490)	77.3	.70	53.7	98.2	1.01	.31	.015	2.08	1,190	.67	2.54	.70937	.24	.24	.7092
ER12–3(4840)	72.1	1.10	53.0	97.2	1.29	> .45	.037	3.89	1,420	.83	5.43	.70928	.11	.11	.7092
ER12–4(2580)	97.9	22.1	30.6	50.0	.66	.18	.036	3.91	146	.30	.29	.71215	4.16	4.73	.7088
ER12–4(3450)	95.0	20.9	33.0	53.2	1.81	> .37	.018	21.5	113	.33	.49	.71007	1.23	2.93	.7080
ER12–4(3590)	98.0	21.4	32.0	51.8	1.77	.41	.020	6.27	133	< .33	< .33	.70847	-1.03	- .04	.7085
ER16–1(3540)	21.9	10.2	26.3	65.0	9.33	>1.50	.179	49.5	327	13.0	3.43	.71485	7.97	9.25	.7083
ER16–1(3800)	69.8	15.2	38.9	64.8	1.36	.33	.036	3.94	70.7	.88	1.55	.71084	2.32	4.16	.7079
HTH–3(1850)	99.0	21.6	30.5	50.4	.19	.01	.009	< .89	16.9	< .26	.29	.70872	- .68	.02	.7087
TW–C(1458)	100.0	10.6	42.4	74.2	.32	.06	.014	< .80	251	< .23	.25	.71072	2.15	3.42	.7083
TW–C(1463.5)	99.5	.99	51.49	97.4	.21	.03	.005	< .96	261	< .28	< .28	.71140	3.10	4.38	.7083
TW–D(1773)	86.8	10.7	40.6	73.2	.51	.18	.052	1.66	454	1.02	.51	.70939	.27	.27	.7092
UE1c(1790)	97.0	.27	51.6	99.3	.23	.03	.005	< .95	405	.63	.74	.70879	- .58	- .02	.7088
UE1c(1860)	77.5	1.15	50.1	96.9	1.02	.44	.150	3.75	327	2.04	.66	.70945	.35	.63	.7090
UE1h(2960)	99.8	22.1	30.5	49.9	.21	.01	.012	<1.00	46.5	< .31	.76	.70811	-1.54	-1.40	.7091
UE2ce(1440)	100.0	21.6	30.5	50.4	.22	.03	.015	< .94	24.3	< .29	< .29	.70854	- .94	- .09	.7086
UE7nS(2052.2)	56.6	.21	52.3	99.4	.65	.26	.050	1.68	292	3.9	.57	.71111	2.70	3.12	.7089
UE7nS(2190)	80.3	.17	52.2	99.6	.39	.10	.036	<1.04	276	.93	.4	.71134	3.02	3.30	.7090
UE10j(1290)	98.3	22.9	29.8	48.4	< .18	.02	.015	< .82	39.2	< .24	< .24	.70870	- .71	- .42	.7090
UE10j(1863)	94.1	22.9	29.4	48.0	.21	.04	.023	< .89	64.9	< .26	.83	.70862	- .82	- .53	.7090
UE10j(2051)	24.5	11.5	19.0	54.4	9.28	>3.87	.170	58	299	27.2	<1.21	.72089	16.49	16.49	.7092
UE10j(2154)	98.9	22.7	29.8	48.5	< .18	.02	.099	< .83	35	< .24	< .24	.70873	- .66	- .52	.7091
UE15d(5960)	97.3	21.6	31.2	51.0	.32	.10	.015	< .80	34.2	< .25	1.19	.71300	5.36	6.49	.7084
UE15d(5994)	96.1	20.4	30.9	52.1	.59	.17	.010	1.96	37.4	<.25	<.25	.71370	6.34	7.48	.7084
UE16d(1020)	98.9	.60	47.0	98.3	.26	.04	.001	<1.02	1,680	< .30	2.18	.70828	-1.30	- .03	.7083
UE16d(1550)	4.1	<1.89	31.5	96.0	6.23	1.68	.234	<22.9	660	<7.04	<7.04	.70889	- .43	.84	.7083

In contrast, three leachate samples with 0.95 to 11.5 weight percent MgO concentrations plot off the calcite-dolomite mixing trend and have elevated SiO_2 concentrations compared to other carbonate leachates (solid squares, fig. 4). These leachates —ER16-1 (3540), UE10j (2051), and UE16d (1550)— also had the lowest percent-sample-dissolved values (4.1 to 24.5 percent) and contained noticeable clay or volcanic constituents. These observations indicate that chemical compositions of these leachates are not derived exclusively from carbonate components and likely include ions leached from silicate minerals.

Measurable amounts of SiO_2 and Al_2O_3 in leachates indicates that small amounts of clay minerals may be present in many of the carbonate samples. The positive correlation between SiO_2 and Al_2O_3 concentrations with a SiO_2:Al_2O_3 weight ratio of 2:1 (fig. 5A) could be the result of variable amounts of clay minerals mixed in with the marine carbonate rocks. Systematic differences in SiO_2 concentrations between dolomite and limestone samples are not apparent (fig. 5B).

Concentrations of Sr vary widely, but systematically, in the carbonate fractions of the 2006 borehole samples (fig. 6). Limestone samples have Sr concentrations ranging from 97.5 to 1,680 micrograms per gram (µg/g) with a median value of 384.5 µg/g (N=16) whereas dolomite samples have Sr concentrations ranging from 16.9 to 146 µg/g with a median value of 46.5 µg/g (N=21). Carbonate samples with $CaCO_3$ mole percentages between 55 and 74 percent have intermediate Sr concentrations with a median value of 140 µg/g (N=11).

Concentrations of Rb in leachates of most samples are less than the minimum reporting limits of around 1 µg/g (table 5). Rb concentrations generally increase with increasing SiO_2 (fig. 7A) indicating that silicate minerals (most likely clays) are a repository of Rb. Dolomite and limestone samples have similar Rb concentrations, but because of their lower Sr concentrations, dolomite samples tend to have higher Rb/Sr ratios (fig. 7B). Most samples have Rb/Sr ratios less than about 0.05. For a Cambrian marine carbonate sample with a Rb/Sr ratio of 0.05 and an initial $^{87}Sr/^{86}Sr$ value of 0.70900 ($\delta^{87}Sr$ = -0.28), the decay of ^{87}Rb during the last 500 m.y. will result in a present-day $^{87}Sr/^{86}Sr$ value of 0.71003 ($\delta^{87}Sr$ = 1.17), an increase of about one in the third decimal place. If the

same rock had a Rb/Sr ratio of 0.015 (the upper limit for most dolomite and limestone samples, fig. 7B), the present-day $^{87}Sr/^{86}Sr$ ratio would only evolve to 0.70931 ($\delta^{87}Sr$ = 0.15). Only four clay-rich samples have Rb/Sr ratios higher than 0.056 (fig. 7B).

Additional elements reported in table 5 include MnO, Th, and U. Concentrations of MnO are statistically uncorrelated with mole percent $CaCO_3$ contents (linear correlation coefficient, r^2, of 0.035) although the highest MnO concentrations are present in limestones. Samples with the lowest SiO_2 concentrations also tend to have the lowest MnO and Th concentrations indicating the potential influence of clay minerals and the low solubility of these constituents in marine environments. In contrast, U concentrations are uncorrelated statistically with SiO_2 and are present in similar concentration ranges in dolomite and limestone samples.

Because CaO and MgO concentrations are not available from XRF analyses, quantification of calcite mole percentages in outcrop samples was not possible. Bulk-rock Sr concentrations range from 16 to 2,537 µg/g with most samples having between about 30 and 500 µg/g (table 6). Samples with Sr concentrations greater than 500 µg/g typically increase along with Zr concentrations (fig. 8A). Because Zr is a highly insoluble element in marine environments (mean Zr concentration in North Pacific Ocean water is 0.000015 µg/g; McKelvey and Orians, 1993) compared to Sr (mean seawater Sr concentration of 7.74 µg/g; Faure and Mensing, 2005, p. 437), Sr concentrations greater than 500 µg/g in outcrop samples likely are attributable to silicate constituents included in the rock. Concentrations of Rb typically cluster at values less than 5 µg/g and are not correlated with Sr concentrations (r^2 value of 0.039 in fig. 8B). However, the crude correlation between Rb and Zr concentration (r^2 value of 0.43 in fig. 8C) implies that both constituents are derived from terrigenous silicate components. Therefore, outcrop samples with the lowest Zr concentrations best represent the carbonate fraction of these bulk-rock analyses. A frequency distribution plot of Sr concentrations in samples having Zr concentrations less than 20 µg/g (fig. 8D) indicates a narrow frequency peak between 25 and 75 µg/g (mostly classified as dolomites in field descriptions) and a broader frequency peak between 100 and 400 µg/g (mostly classified as limestones).
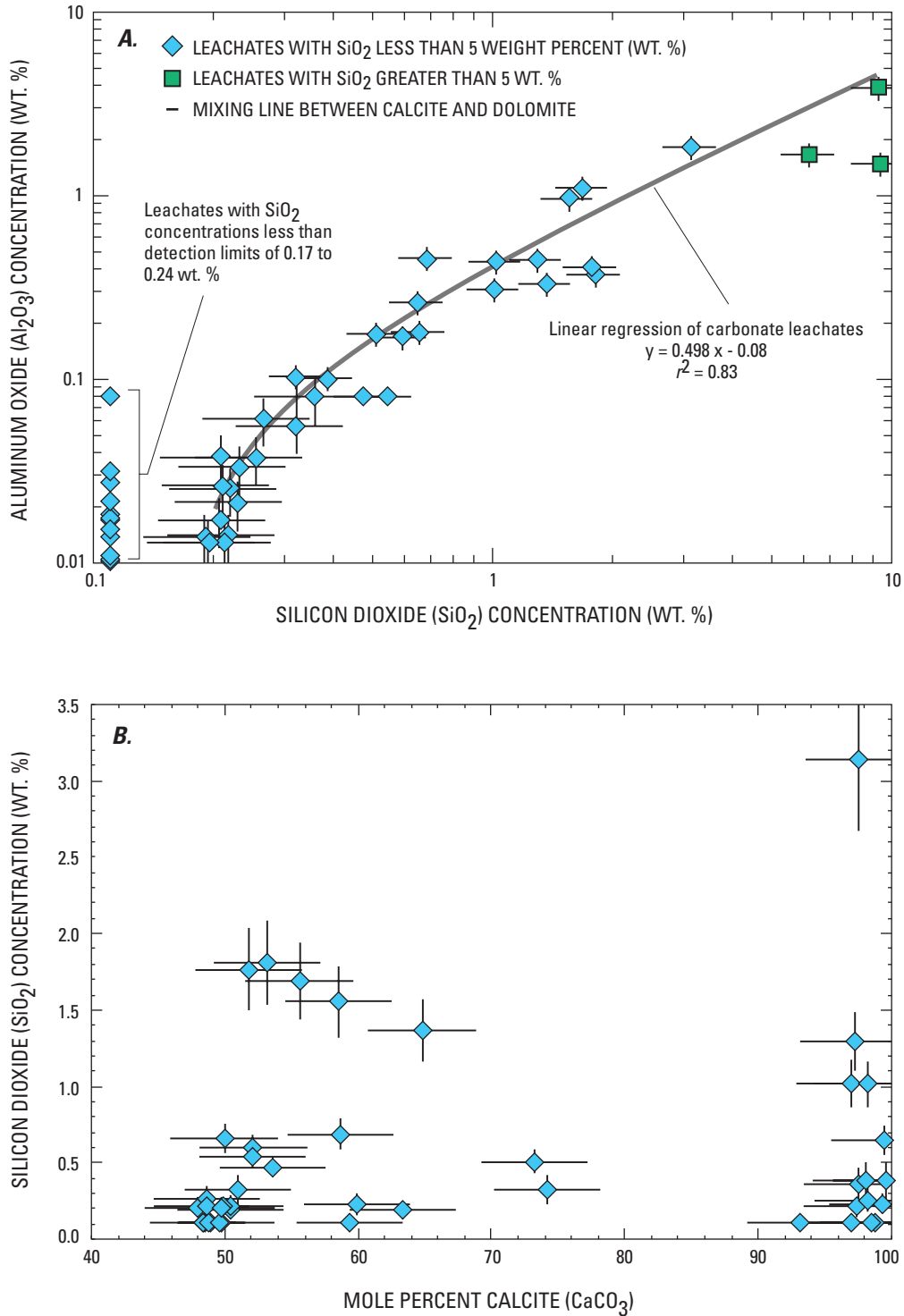
Figure 5.   Relation between (*A*) silicon dioxide (SiO_2) and aluminum oxide (Al_2O_3) concentrations and between (*B*) silicon dioxide and mole percent calcite ($CaCO_3$) in acid leachates of borehole samples, Nevada Test Site, Nye County, Nevada. Error bars represent 2-sigma analytical uncertainty and are shown as 30 percent of the reported concentration value for Al_2O_3 values less than 0.1 wt. % and SiO_2 values less than 0.4 wt. %, and 15 percent for higher concentration values.
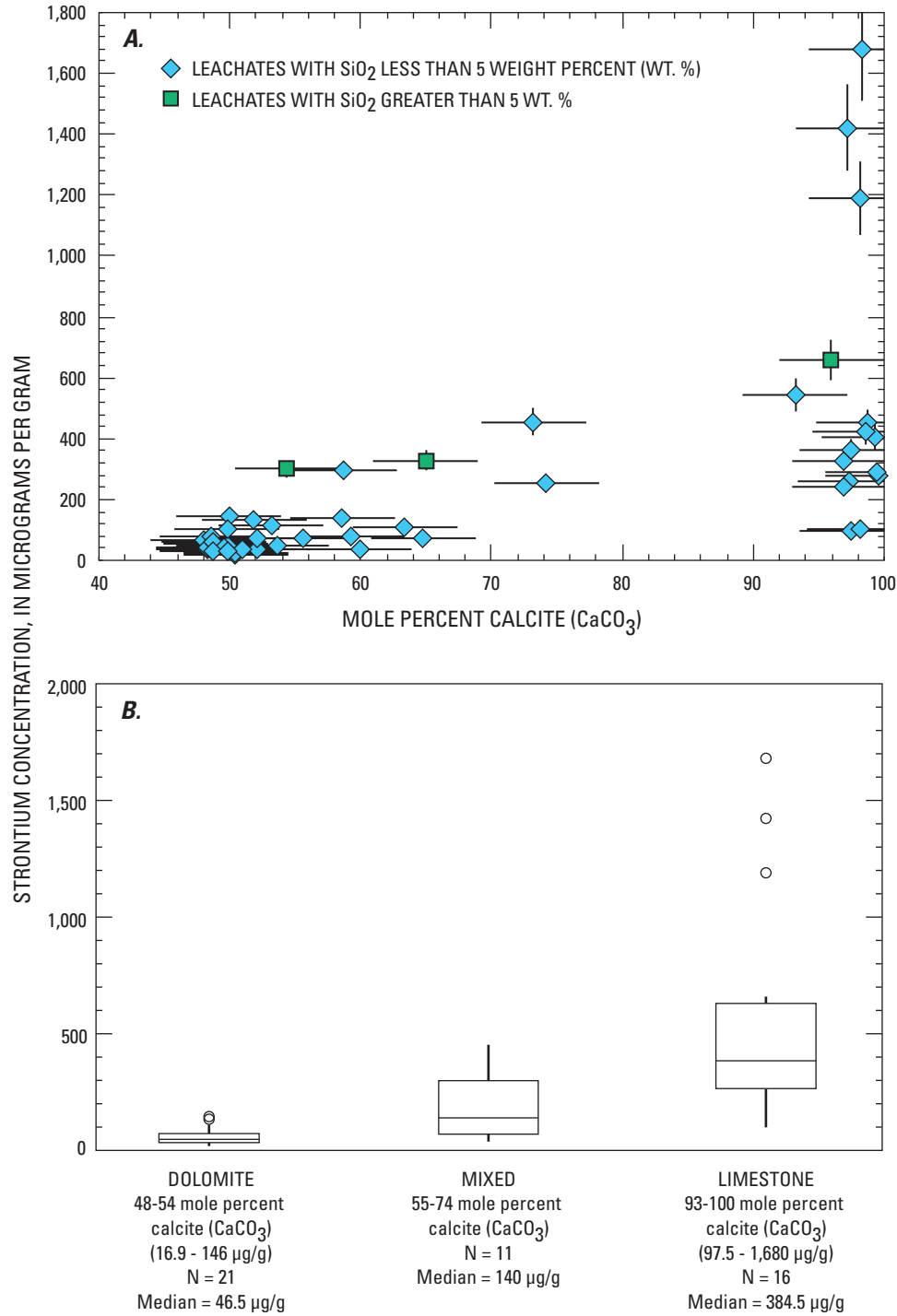
Figure 6.   Relation between (*A*) strontium (Sr) concentration and mole percent calcite ($CaCO_3$) in acid leachates of borehole samples, and (*B*) distribution of strontium concentrations for acid leachates, Nevada Test Site, Nye County, Nevada. Error bars represent 2-sigma analytical uncertainty and are shown as 10 percent of the reported concentration value for strontium and are fixed at 4 mole percent $CaCO_3$.
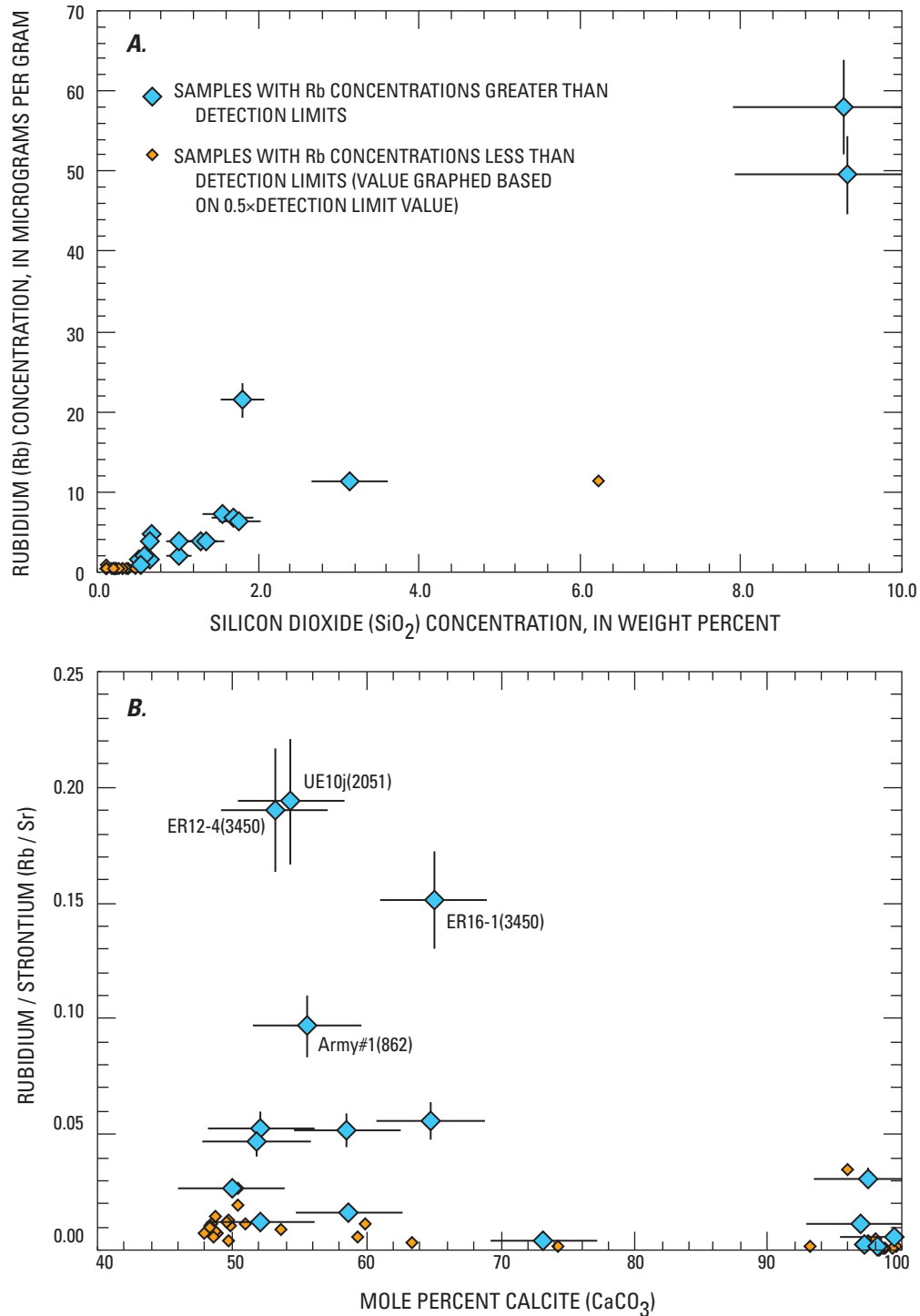
Figure 7. Relation between (*A*) rubidium (Rb) and silicon dioxide (SiO$_2$) concentrations in acid leachates of borehole samples and between (*B*) rubidium/strontium (Rb/Sr) concentration ratios and mole percent calcite (CaCO$_3$) in acid leachates of borehole samples, Nevada Test Site, Nye County, Nevada. Error bars represent 2-sigma analytical uncertainty and are shown as 10 percent of the reported concentration value for rubidium values and 14 percent for rubidium/strontium values. Mole percentages of calcite are shown with fixed 2-sigma analytical uncertainties of 4 mole percent CaCO$_3$.

Table 6.   Bulk-rock analyses of selected trace element concentrations and strontium isotopic compositions ($^{87}Sr/^{86}Sr$) in outcrop samples collected in the early 1990s from the Nevada Test Site vicinity, Clark, Lincoln, and Nye Counties, Nevada, and Inyo County, California.

[Trace element (Rb, Sr, Zr, Ba, La, and Ce) concentrations were determined by X-ray fluorescence on whole-rock samples and are given in micrograms per gram (µg/g). Concentrations below minimum reporting limits are indicated as "0". "ND" indicates that concentrations were not determined. All strontium isotopic compositions ($^{87}Sr/^{86}Sr$) were determined on dilute hydrochloric acid leachates of powdered rock samples with the exception of two samples (map numbers 4 and 5 marked with asterisks) which were determined on whole-rock digestions. $^{87}Sr/^{86}Sr$ uncertainties are typically, but not always, dominated by external error associated with reproducibility of the EN–1 standard (±0.00005). Strontium isotopic compositions are also given in delta notation ($\delta^{87}Sr_t$) = [($^{87}Sr/^{86}Sr_{sample}/^{87}Sr/^{86}Sr_{psw}$)-1]×1,000, where $^{87}Sr/^{86}Sr_{msw}$ is the value for modern seawater and $^{87}Sr/^{86}Sr_{psw}$ is the value for paleoseawater at the time of deposition. $\delta^{87}Sr_t$ values for rocks underlying the Wood Canyon Formation were not calculated (NC) because of the very large uncertainties in assigning ages and initial seawater $^{87}Sr/^{86}Sr$ values, which are designated as "undefined" **Abbreviations and symbols:** Rb, rubidium; Sr, strontium; Zr, zirconium; La, lanthanum; Ce, cerium; ‰, per mil]

Map No.	Sample No.	Rock type	Rb	Sr	Zr	Ba	La	Ce	$^{87}Sr/^{86}Sr$	±2σ	$\delta^{87}Sr$ ‰	±2σ	Unit	$\delta^{87}Sr_t$ ‰	Seawater $^{87}Sr/^{86}Sr_{psw}$ used
1	HD-1106	Calcitic marble	14	1,424	54	0	8	ND	0.70748	0.00005	-2.43	0.07	Yb	NC	Undefined
2	HD-1111	Marble	7	1,453	40	191	0	4	.70727	.00005	-2.72	.07	Yc	NC	Undefined
3	HD-1112	Marble	3.3	1,614	55	187	6	13	.70735	.00005	-2.61	.07	Yc	NC	Undefined
4	HD-1107	Dolomite	4	1,660	47	46	0	0	.70720*	.00005	-2.82	.07	Yb	NC	Undefined
5	HD-1114	Marble	0	2,537	78	11	5	10	.70940*	.00005	.28	.07	Yc	NC	Undefined
6	HD-1105	Dolomite	5	75	31	126	33	60	.71343	.00005	5.97	.07	Zs-c	NC	Undefined
7	HD-1151	Limestone	8	1164	59	25	13	7	.70945	.00005	.35	.07	CZw	1.48	0.7084
8	3C-1	Carbonate	2.5	221	10	30	18	13	.71106	.00005	2.62	.07	Cb	2.76	.7091
9	HD-212	Dolomite	0	146	1	ND	ND	ND	.71181	.00005	3.68	.07	Cb-b	3.68	.7092
10	HD-214	Dolomite	0	211	0	ND	ND	ND	.71279	.00008	5.06	.11	Cb-b	5.06	.7092
11	HD-216	Dolomite	0	256	0	ND	ND	ND	.71125	.00005	2.89	.07	Cb-b	2.89	.7092
12	HD-218	Dolomite	2	152	2	ND	ND	ND	.71201	.00007	3.96	.10	Cb-b	3.96	.7092
13	HD-219	Dolomite	6.8	176	14	ND	ND	ND	.71162	.00005	3.41	.07	Cb-b	3.41	.7092
14	HD-220	Dolomite	1	86	5	ND	ND	ND	.71120	.00005	2.82	.07	Cb-b	2.82	.7092
15	HD-221	Dolomite	0	268	0	ND	ND	ND	.71070	.00005	2.12	.07	Cb-b	2.12	.7092
16	HD-1154	Limestone	24	261	124	180	14	30	.72543	.00005	22.89	.07	CZw-u	24.0	.7084
17	HD-1155	Limestone	7	445	93	47	19	49	.71958	.00005	14.64	.07	CZw	15.8	.7084
18	HD-538	Marble	.6	245	4	45	8	7	.70921	.00005	.01	.07	Cb-p	.30	.7090
19	HD-539	Dolomite	.6	28	0	34	20	16	.70999	.00005	1.11	.07	Cb-p	1.39	.7090
20	HD-540	Dolomite	.6	23	0	31	8	12	.70922	.00005	.03	.07	Cb-p	.31	.7090
21	HD-541	Calcitic marble	2.8	636	27	149	15	37	.72141	.00005	17.21	.07	CZw-u	18.4	.7084
22	HD-513	Dolomite	2.4	96	16	37	28	2	.70946	.00005	.37	.07	Oes	1.35	.7085
23	HD-515	Dolomite	1.3	58	1	42	8	2	.70875	.00005	- .64	.07	Oes	.35	.7085
24	HD-516A	Dolomite	2.4	71	9	42	28	2	.70981	.00008	.86	.11	Sr	1.42	.7088
25	HD-517	Limestone	16	311	36	88	22	16	.71319	.00005	5.63	.07	Sr	6.19	.7088
26	HD-518	Dolomite	7.9	63	31	113	8	12	.71105	.00005	2.61	.07	Sr	3.17	.7088
27	HD-519	Dolomite	1.9	64	0	45	8	10	.70882	.00008	- .54	.11	DSlm	.03	.7088
28	HD-520	Dolomite	.6	55	2	36	11	7	.70861	.00005	- .83	.07	DSlm	.01	.7086
29	HD-533	Limestone	.6	300	11	102	8	2	.71175	.00005	3.6	.07	Op-av	4.02	.7089
30	HD-534	Limestone	4.8	298	6	52	8	9	.71101	.00006	2.55	.08	Op-g	2.69	.7091
31	HD-535	Dolomite	.6	39	0	32	28	2	.70877	.00006	- .61	.08	Cn-s	- .47	.7091
32	HD-1415	Carbonate	0	113	4	0	7	3	.71648	.00005	10.27	.07	Cb-p	10.6	.7090
33	HD-1416	Carbonate	0	177	5	0	13	0	.71323	.00005	5.68	.07	Cb-p	5.97	.7090
34	HD-1417	Carbonate	0	979	47	34	12	38	.71829	.00005	12.82	.07	CZw-l	14.0	.7084
35	HD-1418	Carbonate	0	151	2	0	0	0	.72260	.00005	18.9	.07	CZw-l	20.0	.7084
36	HD-1419	Carbonate	0	166	4	2	15	11	.72327	.00005	19.84	.07	Cb-p	20.1	.709
37	HD-1420	Carbonate	0	66	1	0	6	0	.71905	.00005	13.89	.07	Cb-p	14.2	.709
38	HD-1421	Carbonate	2.8	627	28	47	13	31	.71374	.00005	6.40	.07	CZw-l	7.54	.7084
39	HD-527	Dolomite	.6	47	0	25	18	10	.70816	.00007	-1.47	.10	Df	.37	.7079
40	HD-528	Dolomite	1.1	60	0	39	8	11	.71152	.00005	3.27	.07	Df	5.11	.7079
41	HD-529	Calcitic marble	3	166	0	41	8	2	.71017	.00005	1.36	.07	Cb-b	1.36	.7092
42	HD-530	Dolomitic marble	.6	27	0	33	16	2	.70927	.00005	.10	.07	Cb-b	.10	.7092

Table 6. Bulk-rock analyses of selected trace element concentrations and strontium isotopic compositions ($^{87}Sr/^{86}Sr$) in outcrop samples collected in the early 1990s from the Nevada Test Site vicinity, Clark, Lincoln, and Nye Counties, Nevada, and Inyo County, California.—Continued

[Trace element (Rb, Sr, Zr, Ba, La, and Ce) concentrations were determined by X-ray fluorescence on whole-rock samples and are given in micrograms per gram (μg/g). Concentrations below minimum reporting limits are indicated as "0". "ND" indicates that concentrations were not determined. All strontium isotopic compositions ($^{87}Sr/^{86}Sr$) were determined on dilute hydrochloric acid leachates of powdered rock samples with the exception of two samples (map numbers 4 and 5 marked with asterisks) which were determined on whole-rock digestions. $^{87}Sr/^{86}Sr$ uncertainties are typically, but not always, dominated by external error associated with reproducibility of the EN–1 standard (±0.00005). Strontium isotopic compositions are also given in delta notation ($\delta^{87}Sr_t$) = [($^{87}Sr/^{86}Sr_{sample}/^{87}Sr/^{86}Sr_{psw}$)-1]×1,000, where $^{87}Sr/^{86}Sr_{msw}$ is the value for modern seawater and $^{87}Sr/^{86}Sr_{psw}$ is the value for paleoseawater at the time of deposition. $\delta^{87}Sr_t$ values for rocks underlying the Wood Canyon Formation were not calculated (NC) because of the very large uncertainties in assigning ages and initial seawater $^{87}Sr/^{86}Sr$ values, which are designated as "undefined" **Abbreviations and symbols:** Rb, rubidium; Sr, strontium; Zr, zirconium; La, lanthanum; Ce, cerium; ‰, per mil]

Map No.	Sample No.	Rock type	Rb	Sr	Zr	Ba	La	Ce	$^{87}Sr/^{86}Sr$	±2σ	$\delta^{87}Sr$ ‰	±2σ	Unit	$\delta^{87}Sr_t$ ‰	Seawater $^{87}Sr/^{86}Sr_{psw}$ used
43	HD-531	Calcitic marble	4.2	403	13	50	8	2	0.70960	0.00005	0.56	0.07	Cn-h	0.56	0.7092
44	HD-542	Dolomitic marble	4.5	371	8	39	20	28	.71010	.00005	1.27	.07	CZw-l	2.40	.7084
45	HD-543	Dolomite	.6	200	2	39	16	21	.71551	.00005	8.90	.07	Cb-p	9.19	.7090
46	HD-1152b	Altered limestone	4	98	16	11	5	9	.71150	.00005	3.24	.07	Zs-d	NC	Undefined
47	HD-1153	Limestone	3	306	12	13	14	25	.71125	.00005	2.89	.07	Zs-d	NC	Undefined
48	HD-1142	Limestone	6	390	18	29	0	0	.70876	.00005	- .62	.07	Op-g	- .20	.7089
49	HD-1144	Limestone	2	35	14	58	14	0	.70935	.00005	.21	.07	Df	2.04	.7079
50	HD-1400	Carbonate	0	56	0	0	12	8	.71265	.00005	4.87	.07	Cb-b	4.87	.7092
51	HD-1401	Carbonate	1.4	70	3	0	15	10	.71289	.00005	5.20	.07	Cb-b	5.2	.7092
52	HD-1402	Carbonate	0	67	1	0	13	0	.71173	.00005	3.57	.07	Cb-b	3.57	.7092
53	HD-641	Carbonate	0	62	7	0	20	25	.71703	.00008	11.04	.11	Cb-b	11.0	.7092
54	HD-537	Dolomite	9.1	115	29	61	36	66	.71275	.00005	5.01	.07	Zs-d	NC	Undefined
55	HD-1146	Limestone	0	283	8	147	4	0	.71292	.00005	5.25	.07	MDe	6.95	.7080
56	HD-1147a	Limestone	14	197	20	140	8	12	.70926	.00005	.09	.07	Dtc	.66	.7088
57	HD-1147b	Limestone	2	120	5	23	6	7	.71088	.00005	2.37	.07	Dtc	2.93	.7088
58	HD-522	Dolomite	1.3	63	0	101	29	27	.70976	.00008	.79	.11	Dtc	1.35	.7088
59	HD-523	Limestone	6.7	172	7	141	8	13	.71029	.00005	1.53	.07	Dtc	2.10	.7088
60	HD-526	Limestone	2.5	668	20	55	13	6	.71018	.00007	1.38	.10	Cc-m	2.37	.7085
61	HD-1138	Limestone	9	777	40	37	12	0	.70884	.00005	-.51	.07	Op-av	-.09	.7089
62	HD-1139	Dolomite/ limestone	2	65	20	0	16	0	.70935	.00005	.22	.07	DSlm	.78	.7088
63	HD-1141	Limestone	10	1,140	54	57	14	0	.70906	.00005	- .2	.07	Op-av	.22	.7089
64	HD-1150b	Carbonate	7	507	25	38	7	22	.71722	.00005	11.31	.07	CZw	12.5	.7084
65	HD-546	Dolomite	.6	45	0	36	25	24	.70886	.00006	- .48	.08	Dsi	1.36	.7079
66	HD-548	Limestone	8.5	382	8	42	17	18	.70921	.00007	.01	.10	Op-av	.44	.7089
67	HD-549	Limestone	10.6	315	10	82	8	11	.70979	.00005	.83	.07	Op-g	.97	.7091
68	HD-550	Limestone	3.7	297	7	45	23	13	.70921	.00005	.01	.07	Op-g	.16	.7091
69	HD-551A	Dolomite	.6	47	1	30	19	19	.70929	.00005	.13	.07	Op-g	.27	.7091
70	HD-553	Limestone	4.2	631	22	48	12	2	.71013	.00005	1.31	.07	Cn-h	1.31	.7092
71	HD-554	Limestone	.6	496	9	42	8	8	.70937	.00005	.24	.07	Cb-b	.24	.7092
72	HD-555	Limestone	2.1	348	10	44	16	16	.70936	.00005	.23	.07	Cb-b	.23	.7092
73	HD-556	Limestone	3.2	362	9	50	8	7	.70938	.00005	.25	.07	Cb-b	.25	.7092
74	HD-557	Limestone	1.9	207	3	36	15	2	.70912	.00005	- .11	.07	Cb-p	.03	.7091
75	HD-558	Limestone	5.2	442	5	32	8	2	.70918	.00007	- .03	.10	Cb-p	.11	.7091
76	HD-1422-1	Carbonate	30.2	528	74	118	11	14	.71255	.00005	4.72	.07	Cb-b	4.72	.7092
77	HD-1422-2	Carbonate	3	247	14	17	4	17	.71103	.00005	2.58	.07	Cb-b	2.58	.7092
78	HD-1423	Carbonate	19.6	204	51	82	16	0	.71003	.00005	1.17	.07	Cb-b	1.17	.7092
79	HD-1426	Carbonate	1.4	145	18	8	19	38	.71243	.00005	4.56	.07	CZw	5.55	.7085
80	HD-1427	Carbonate	3.8	334	20	10	0	0	.70937	.00005	.24	.07	Cb-b	.24	.7092
81	HD-1428	Carbonate	0	175	5	0	6	5	.70899	.00005	- .30	.07	Cb-b	- .16	.7091
82	HD-1429	Carbonate	3.3	292	14	10	9	4	.70911	.00005	- .13	.07	Cb-b	.01	.7091
83	HD-1432	Carbonate	1.9	555	21	9	12	11	.70931	.00005	.16	.07	Cn	.30	.7091

Table 6.   Bulk-rock analyses of selected trace element concentrations and strontium isotopic compositions ($^{87}Sr/^{86}Sr$) in outcrop samples collected in the early 1990s from the Nevada Test Site vicinity, Clark, Lincoln, and Nye Counties, Nevada, and Inyo County, California.—Continued

[Trace element (Rb, Sr, Zr, Ba, La, and Ce) concentrations were determined by X-ray fluorescence on whole-rock samples and are given in micrograms per gram (µg/g). Concentrations below minimum reporting limits are indicated as "0". "ND" indicates that concentrations were not determined. All strontium isotopic compositions ($^{87}Sr/^{86}Sr$) were determined on dilute hydrochloric acid leachates of powdered rock samples with the exception of two samples (map numbers 4 and 5 marked with asterisks) which were determined on whole-rock digestions. $^{87}Sr/^{86}Sr$ uncertainties are typically, but not always, dominated by external error associated with reproducibility of the EN–1 standard (±0.00005). Strontium isotopic compositions are also given in delta notation ($\delta^{87}Sr_t$) = [($^{87}Sr/^{86}Sr_{sample}/^{87}Sr/^{86}Sr_{psw}$)-1]×1,000, where $^{87}Sr/^{86}Sr_{msw}$ is the value for modern seawater and $^{87}Sr/^{86}Sr_{psw}$ is the value for paleoseawater at the time of deposition. $\delta^{87}Sr_t$ values for rocks underlying the Wood Canyon Formation were not calculated (NC) because of the very large uncertainties in assigning ages and initial seawater $^{87}Sr/^{86}Sr$ values, which are designated as "undefined" **Abbreviations and symbols:** Rb, rubidium; Sr, strontium; Zr, zirconium; La, lanthanum; Ce, cerium; ‰, per mil]

| Map No.	Sample No.	Rock type	Rb	Sr	Zr	Ba	La	Ce	$^{87}Sr/^{86}Sr$	±2σ	$\delta^{87}Sr$ ‰	±2σ	Unit	$\delta^{87}Sr_t$ ‰	Seawater $^{87}Sr/^{86}Sr_{psw}$ used
84	HD-1434	Carbonate	0	51	0	0	17	8	0.70804	0.00005	-1.64	0.07	Dsv	0.06	0.7080
85	HD-1435	Marble	1	501	21	13	7	14	.71282	.00005	5.10	.07	Cc	6.09	.7085
86	HD-1436	Carbonate	2	140	6	0	12	24	.70922	.00005	.03	.07	Cb-b	.03	.7092
87	HD-110-1	Limestone	5	312	20	ND	ND	ND	.70990	.00005	.99	.07	Cb-b	.99	.7092
88	HD-471B	Carbonate	10.7	345	36	107	21	15	.70980	.00009	.85	.13	Cb-b	.85	.7092
89	GDR-8	Carbonate	2	275	5	ND	ND	ND	.70913	.00005	- .10	.07	PMb	1.17	.7083
90	HD-229	Limestone	0	743	9	ND	ND	ND	.70831	.00005	-1.26	.07	PMbl	.01	.7083
91	HD-230	Limestone	0	132	0	ND	ND	ND	.70827	.00005	-1.31	.07	PMbl	- .04	.7083
92	HD-231	Limestone	2	564	2	ND	ND	ND	.70844	.00005	-1.07	.07	Mm	.34	.7082
93	HD-232	Limestone	0	25	0	ND	ND	ND	.70857	.00005	- .89	.07	Cb-b	- .75	.7091
94	HD-233	Limestone	0	28	0	ND	ND	ND	.70933	.00008	.18	.11	Cb-b	.18	.7092
95	HD-235	Limestone	0	29	0	ND	ND	ND	.70847	.00007	-1.03	.10	Cn	- .75	.7090
96	HD-236	Limestone	0	66	6	ND	ND	ND	.70859	.00007	- .86	.10	Op	- .01	.7086
97	HD-238	Limestone	8	263	82	ND	ND	ND	.70790	.00005	-1.83	.07	PMb	.00	.7079
98	HD-1000	Limestone	1	104	6	14	9	0	.70834	.00005	-1.21	.07	Dg	.06	.7083
99	HD-999	Dolomite	3	29	13	32	18	0	.70881	.00005	- .55	.07	Cn-s	- .27	.7090
100	HD-995	Dolomite	0	67	4	22	15	9	.70845	.00005	-1.06	.07	Oes	.21	.7083
101	HD-996	Dolomite	2	327	14	25	18	13	.70912	.00005	- .12	.07	Op-av	.17	.7090
102	HD-997	Dolomite	0	422	15	19	7	0	.70884	.00005	- .51	.07	Oes	.76	.7083
103	HD-998	Limestone	3	345	11	43	0	0	.70880	.00005	- .56	.07	Op-av	.01	.7088
104	HD-1001	Dolomite	1	233	9	29	5	0	.70912	.00005	- .12	.07	Op-av	.17	.7090
105	HD-1006	Limestone	1	16	42	10	14	0	.70918	.00005	- .02	.07	Op-av	.12	.7091
106	HD-990	Limestone	2	56	6	13	8	0	.70841	.00005	-1.11	.07	Op-av	- .12	.7085
107	HD-1002	Dolomite	1	44	5	11	14	0	.70853	.00005	- .95	.07	Oes	.32	.7083
108	HD-991	Dolomite	1	63	2	5	8	13	.70813	.00005	-1.51	.07	Oes	.04	.7081
109	HD-993	Dolomite	0	22	0	30	9	14	.70862	.00005	- .82	.07	Dsi	1.01	.7079
110	HD-994	Limestone	0	470	15	42	13	0	.70817	.00005	-1.45	.07	Mj	.10	.7081
111	HD-1004	Limestone	4	204	85	38	17	10	.70884	.00005	- .50	.07	Op-av	- .08	.7089
112	HD-1003	Limestone	4	164	13	20	0	0	.70826	.00005	-1.32	.07	Dg	- .05	.7083
113	HD-1007	Limestone	2	258	22	19	13	18	.70994	.00005	1.04	.07	Op-g	1.18	.7091
114	HD-1008	Dolomite	9	59	32	29	0	0	.70915	.00005	- .07	.07	Dsv	.49	.7088
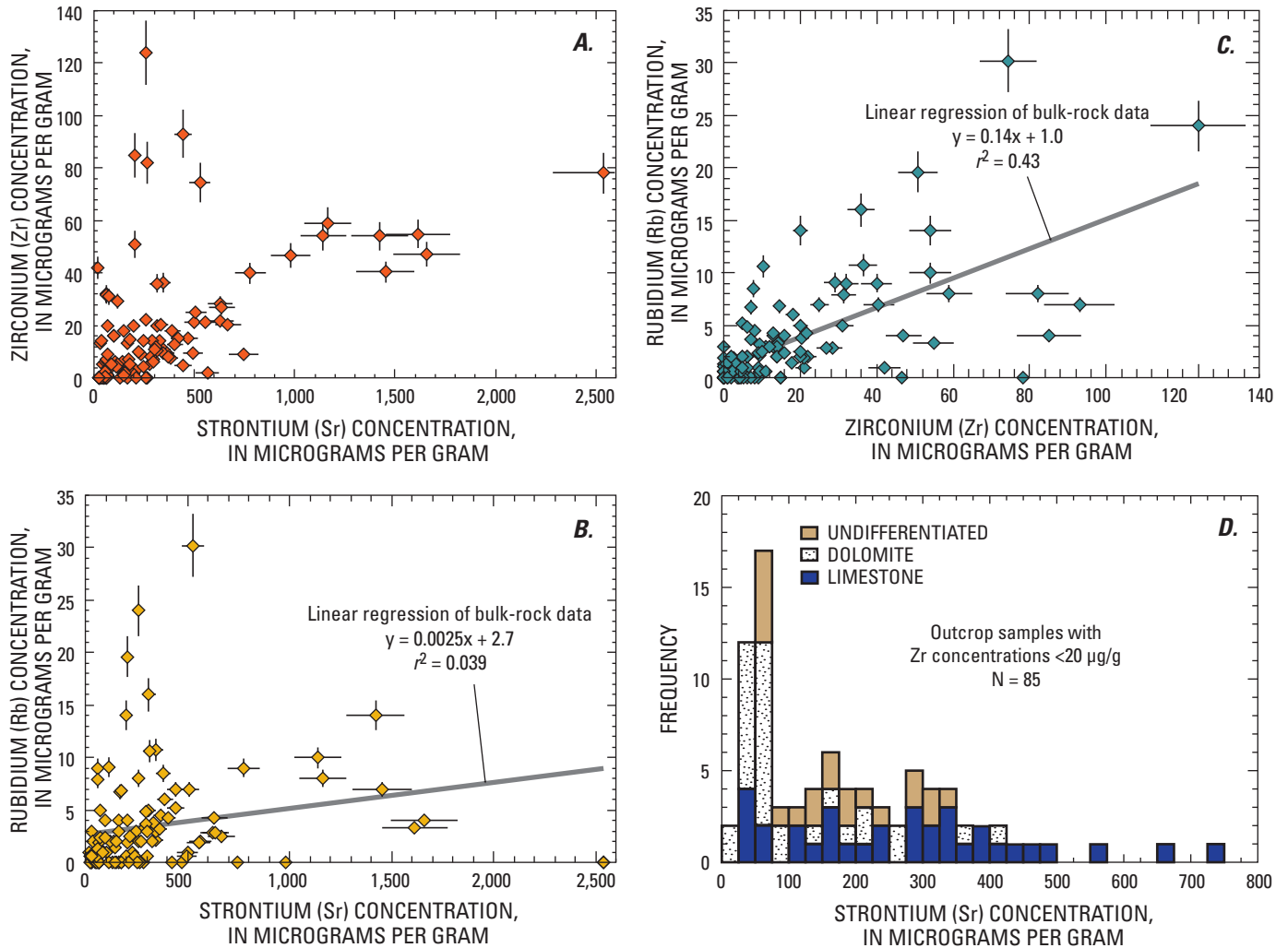
Figure 8. Relation between (*A*) strontium (Sr) and zirconium (Zr) concentrations, (*B*) strontium and rubidium (Rb) concentrations, (*C*) zirconium and rubidium concentrations for bulk-rock outcrop samples, and (*D*) the frequency distribution of strontium concentrations for bulk-rock outcrop samples with zirconium concentrations less than or equal to 20 micrograms per gram, Nevada Test Site and adjacent areas, Clark, Lincoln, and Nye Counties, Nevada, and Inyo County, California. Error bars represent 2-sigma analytical uncertainty and are shown as 10 percent of the reported concentration value.

Strontium Isotopic Compositions

Values of $^{87}Sr/^{86}Sr$ for the carbonate fractions of borehole (tables 5 and 7), and outcrop (table 6) samples range from 0.70720 to 0.72543 and have distributions that are skewed toward radiogenic values (fig. 9). For both sets of samples, approximately 54 percent of the $^{87}Sr/^{86}Sr$ analyses are within the range of Paleozoic seawater values between 0.7070 and 0.7092. The remaining analyses have larger $^{87}Sr/^{86}Sr$ values, typically between 0.7093 and 0.7150. Data from Yucca Flat core and cutting samples do not form linear trends on plots

comparing $^{87}Sr/^{86}Sr$ to reciprocal Sr concentration (fig. 10*A*) where binary mixing trends would plot as straight lines. Therefore, there is no indication that low Sr carbonates were more susceptible to addition of radiogenic Sr from secondary fluids than high Sr samples. Furthermore, there are no clear indications that elevated $^{87}Sr/^{86}Sr$ values in carbonate fractions are related to the presence of Rb-rich silicate components leached from the samples (fig. 10*B*). Although the two clay-rich samples with the highest SiO_2 concentrations also have the highest $^{87}Sr/^{86}Sr$ values, similar trends are not present in samples with lower SiO_2 concentrations.

Table 7.   Selected trace element concentrations and strontium isotopic compositions ($^{87}Sr/^{86}Sr$) in core samples from boreholes UE-25 a #3 and UE-25 p #1, Nevada Test Site, Nye County, Nevada.

[Siliciclastic lithologies for samples from surface to 697.2-m depth in borehole UE–25 a #3 consist of Mississippian (middle Chester to early Osage stages) Chainman Shale and Gap Wash Formation (Maldonado and others, 1979; Cole and Cashman, 1998). Underlying core is undifferentiated Devonian carbonate (Du). Stratigraphic units for borehole UE–25 p #1 are from Carr and others (1986). **Stratigraphic unit** symbols are defined in table 1. **Analysis type:** WR indicates that strontium isotopic compositions ($^{87}Sr/^{86}Sr$) were determined on whole-rock digestions using concentrated hydrofluoric, nitric, hydrochloric, and sulfuric acids; HCl–L indicates that $^{87}Sr/^{86}Sr$ values were determined on dilute hydrochloric acid leachates of powdered rock samples. Strontium isotopic compositions also are given in delta notation ($\delta^{87}Sr = [(^{87}Sr/^{86}Sr_{sample}/^{87}Sr/^{86}Sr_{msw})-1]\times1,000$ and $\delta^{87}Sr_t = [(^{87}Sr/^{86}Sr_{sample}/^{87}Sr/^{86}Sr_{psw})-1]\times1,000$, where $^{87}Sr/^{86}Sr_{msw}$ is the value for modern seawater and $^{87}Sr/^{86}Sr_{psw}$ is the value for paleoseawater at the time of deposition). **Abbreviations and symbols:** Rb, rubidium; Sr, strontium; Y, yittrium; Zr, zirconium; Nb, Niobium; Ba, barium; La, lanthanum; Ce, cerium; m, meter; ‰, per mil; ND, not determined]

Sample identification No.	Borehole	Borehole depth (m)	Strati- graphic unit	Rb	Sr	Y	Zr	Nb	Ba	La	Ce	Analysis type	$^{87}Sr/^{86}Sr$ (±0.00005 2σ)	$\delta^{87}Sr$, ‰ (±0.07 2σ)	$\delta^{87}Sr_t$ ‰	Seawater $^{87}Sr/^{86}Sr_{psw}$ used
UE25a3–142	UE–25 a #3	43.3	Mc/MDg	48	89	45	320	16	115	ND	ND	WR	0.71554	8.94	10.4	0.7082
UE25a3–324	UE–25 a #3	98.8	Mc/MDg	90	176	41	173	20	182	ND	ND	WR	.71616	9.81	11.4	.7081
UE25a3–493	UE–25 a #3	150.4	Mc/MDg	54	91	42	282	20		ND	ND	WR	.71795	12.34	14.0	.7080
UE25a3–684	UE–25 a #3	208.4	Mc/MDg	84	177	44	212	21	210	ND	ND	WR	.71539	8.73	10.5	.7079
UE25a3–863	UE–25 a #3	263.1	Mc/MDg	77	159	49	273	19	189	ND	ND	WR	.71523	8.50	10.5	.7078
UE25a3–1069	UE–25 a #3	325.7	Mc/MDg	80	205	43	189	20	240	ND	ND	WR	.71494	8.09	10.2	.7077
UE25a3–1430	UE–25 a #3	435.9	Mc/MDg	78	74	27	117	9	1,247	ND	ND	WR	.71633	10.05	12.2	.7077
UE25a3–1722	UE–25 a #3	525.0	Mc/MDg	146	65	32	151	14	1,575	ND	ND	WR	.72022	15.54	17.4	.7079
UE25a3–1846	UE–25 a #3	562.5	Mc/MDg	61	86	26	137	15	889	ND	ND	WR	.72087	16.46	18.3	.7080
UE25a3–2093	UE–25 a #3	637.9	Mc/MDg	39	51	15	96	6	394	ND	ND	WR	.72369	20.43	22.1	.7081
UE25a3–2287	UE–25 a #3	697.2	Mc/MDg	71	131	31	176	7	299	ND	ND	WR	.71700	11.00	12.5	.7082
UE25a3–2432	UE–25 a #3	741.1	Du	2	87	33	6	2		ND	ND	WR	.71323	5.68	7.10	.7082
UE25a3–2492	UE–25 a #3	759.6	Du	0	60	5	3	0	73	21	3	HCl-L	.71111	2.69	4.04	.7083
UE25a3–2514	UE–25 a #3	766.4	Du	0	36	5	2	0	38	24	6	HCl-L	.71080	2.26	3.60	.7083
HD–622	UE–25 p #1	1,277.7	DSlm	0	68	0	14	0	10	5	11	HCl-L	.70907	- .19	.38	.7088
HD–621	UE–25 p #1	1,284.1	DSlm	0	62	0	11	0	0	9	0	HCl-L	.70905	- .21	.35	.7088
UE25p 1–5900	UE–25 p #1	1,798.3	Sr	3	70	5	15	0	0	23	14	HCl-L	.70835	-1.20	- .07	.7084

Values of $\delta^{87}Sr_t$ calculated with respect to the estimates for Paleozoic seawater $^{87}Sr/^{86}Sr$ at the time of deposition range widely from -1.40 to 24.0 (tables 5–7; fig. 11). Estimates for the original seawater $^{87}Sr/^{86}Sr$ were made using the lithostratigraphic age assignments (table 1) and the Paleozoic seawater $^{87}Sr/^{86}Sr$ curve of McArthur and others (2001; fig. 3). In many cases, specific age and Paleozoic seawater $^{87}Sr/^{86}Sr$ values for individual samples were chosen from the ranges permissible in table 1 to obtain a $\delta^{87}Sr_t$ value closer to 0.0. Although the Paleozoic seawater $^{87}Sr/^{86}Sr$ evolution curve is well established, error bars are not shown on figure 11 because of the difficulty in defining uncertainties for rock ages based on stratigraphic intervals that can span ranges of 10–50 m.y. or more. Values of $\delta^{87}Sr_t$ close to 0.0 indicate that the carbonate rocks likely have retained their original Paleozoic marine Sr isotopic signatures. In some cases, these data may help corroborate age assignments based on biostratigraphic information (Banner, 2004, p. 167). However, it is preferable to obtain $^{87}Sr/^{86}Sr$ data from low-magnesium calcite constituting marine skeletons instead of from bulk rock to avoid post-depositional alteration (Veizer and others, 1999, p. 62). Because all analyses reported here were done on bulk-rock samples, no attempts are made to refine depositional ages.
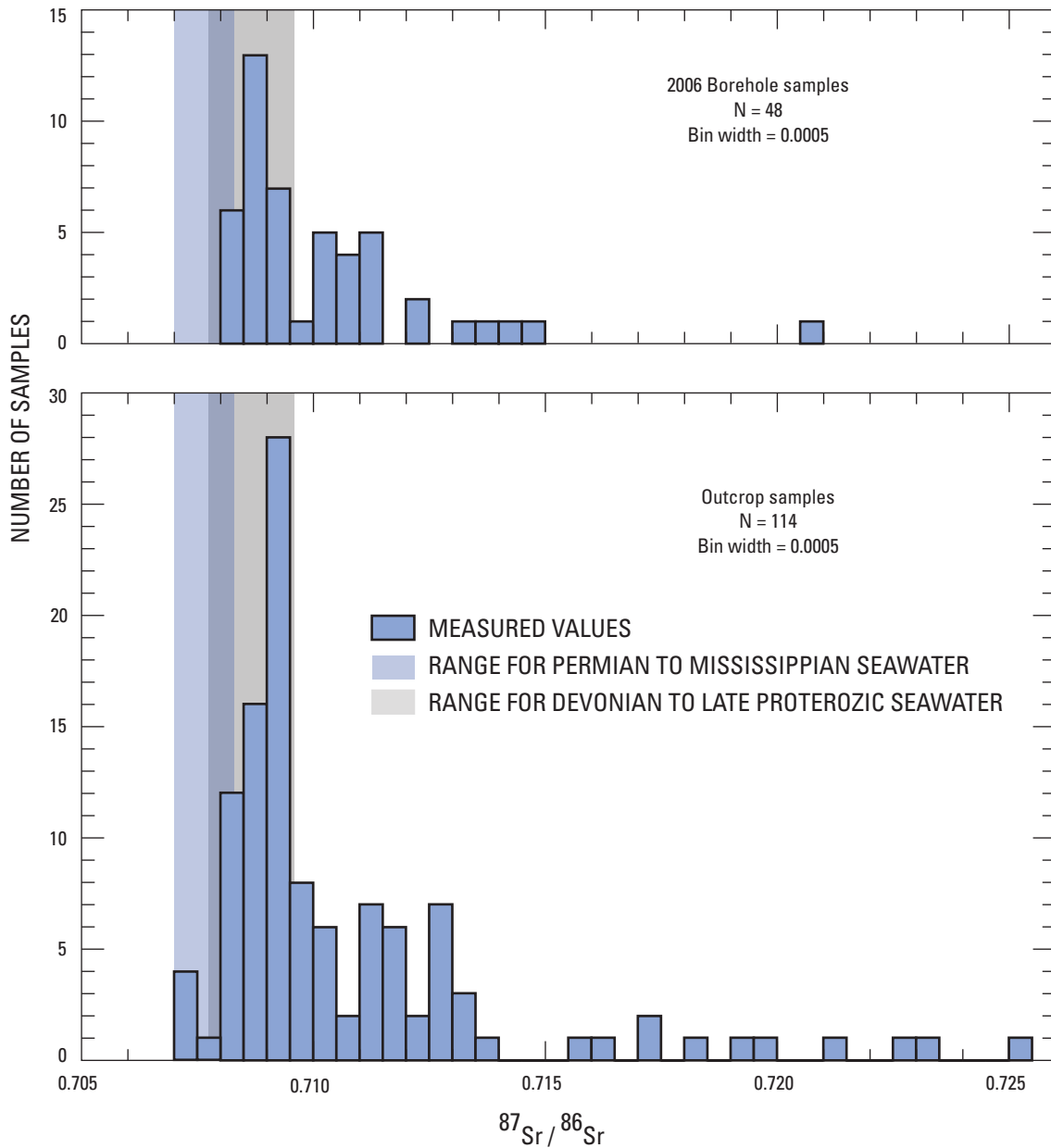
Figure 9.   Distribution of strontium isotopic compositions ($^{87}Sr/^{86}Sr$) measured in borehole and outcrop samples, Nevada Test Site and adjacent areas, Clark, Lincoln, and Nye Counties, Nevada, and Inyo County, California. Permian and Pennsylvanian carbonates constituting the upper carbonate aquifer at the Nevada Test Site (fig. 2) typically have lower $^{87}Sr/^{86}Sr$ values than the older Paleozoic carbonates constituting the lower carbonate aquifer ($^{87}Sr/^{86}Sr$ ranges from figure 3).
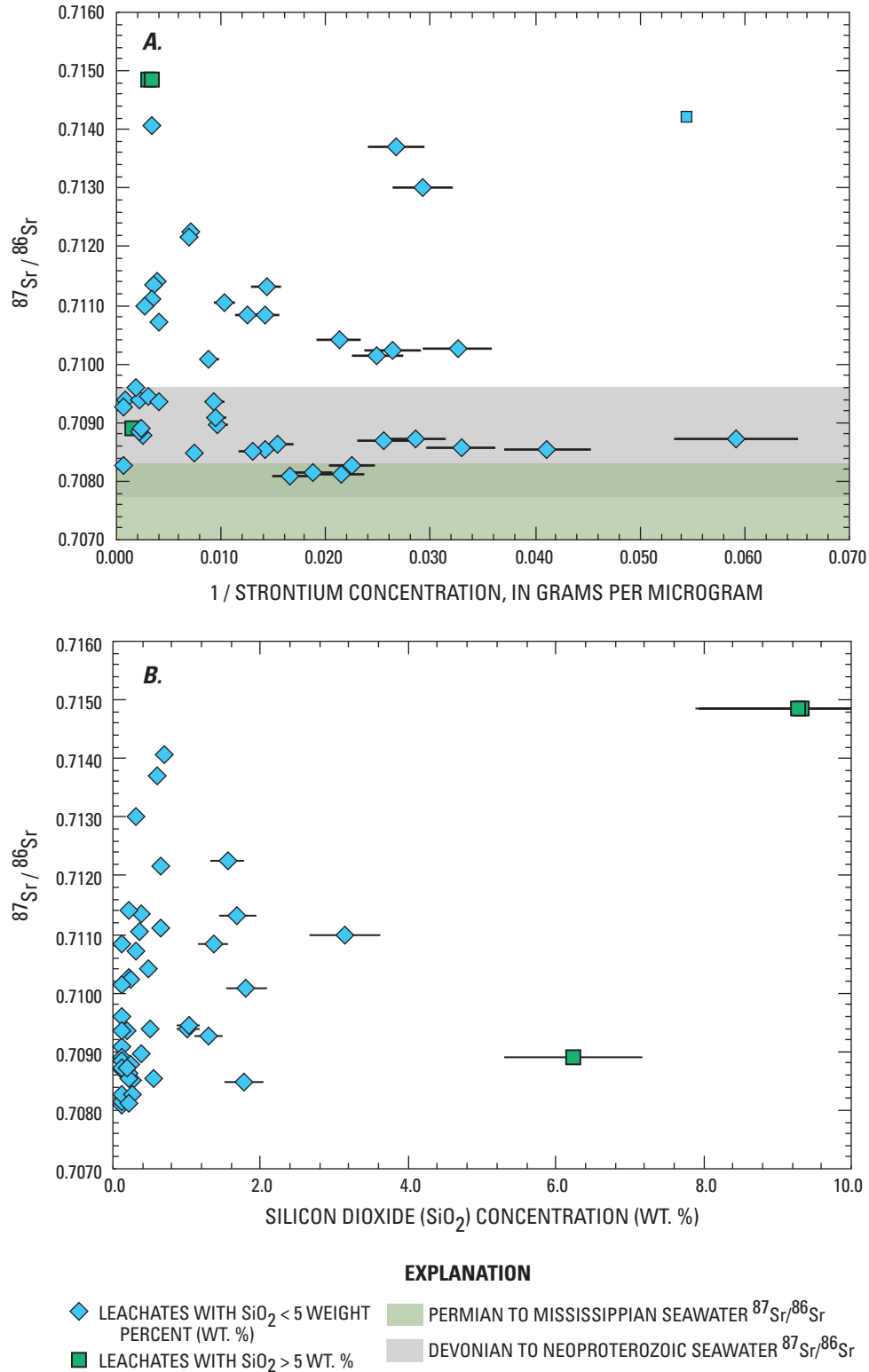
Figure 10. Relation between (*A*) strontium isotopic compositions ($^{87}Sr/^{86}Sr$) and reciprocal strontium concentrations for acid leachates of borehole samples and (*B*) $^{87}Sr/^{86}Sr$ and silicon dioxide (SiO_2) concentrations for acid leachates of borehole samples, Nevada Test Site, Nye County, Nevada. Error bars represent 2-sigma analytical uncertainty and are shown as 10 percent of the reported concentration value for strontium and 15 percent for SiO_2.
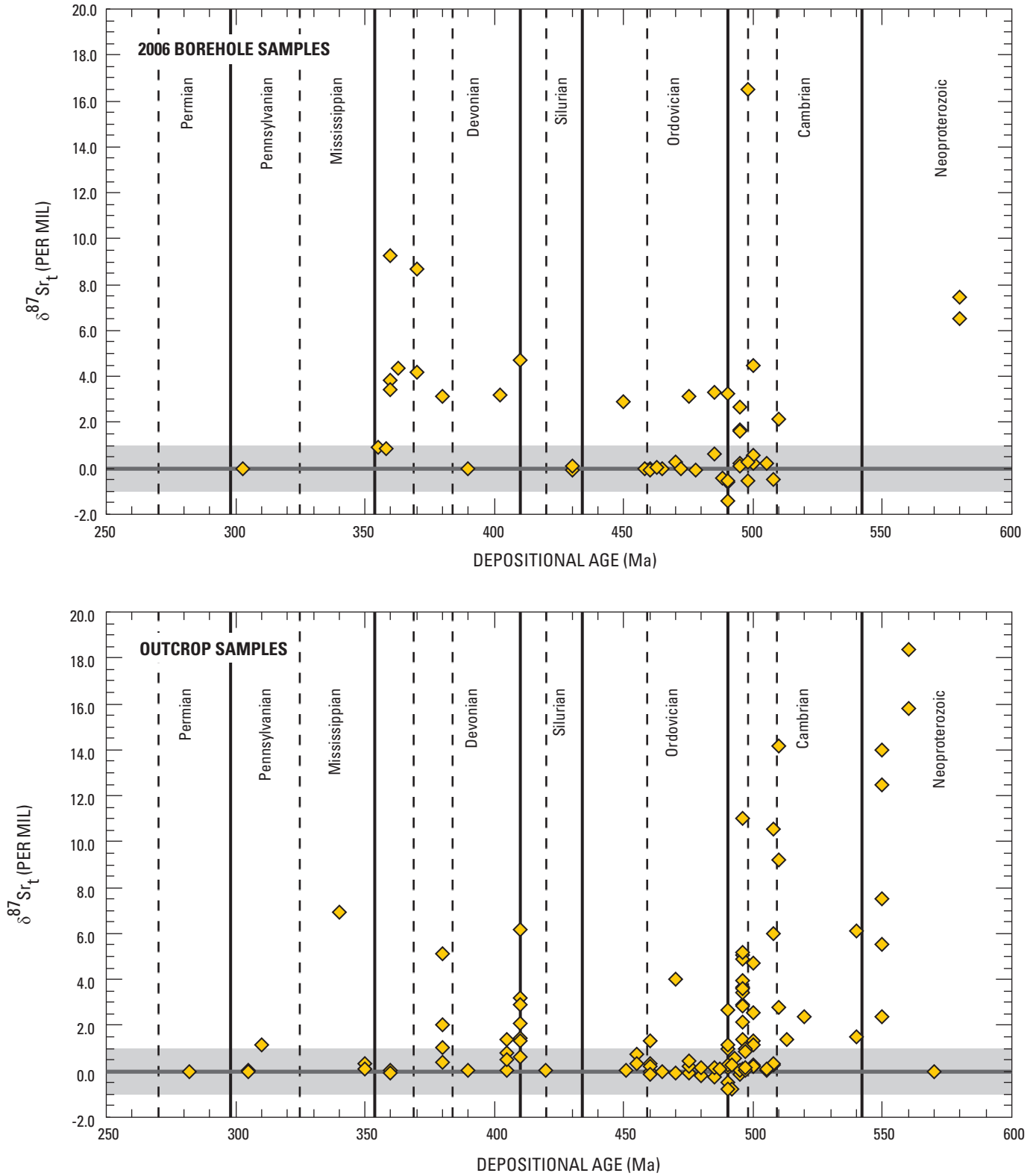
Figure 11. Relation between $\delta^{87}Sr_t$, and depositional age for acid leachates of borehole and outcrop samples, Nevada Test Site and adjacent areas, Clark, Lincoln, and Nye Counties, Nevada, and Inyo County, California. Data are from tables 5 and 6. Four analyses with $\delta^{87}Sr_t$ values between 20.0 and 24.0 are not shown. Shaded band depicts ±1 per mil deviation from the assumed paleoseawater value and is shown for reference.

Samples with measured $^{87}Sr/^{86}Sr$ values greater than 0.7093 in tables 5–7 have undergone obvious post-depositional addition of radiogenic Sr (Peterman and others, 1994). Samples with elevated $\delta^{87}Sr_t$ are present throughout the Paleozoic stratigraphic section in borehole and outcrop samples (fig. 11), indicating that $^{87}Sr/^{86}Sr$ alteration was not restricted to rocks formed during a narrow interval of Paleozoic time. Peterman and others (1994) documented that Paleozoic carbonates at Bare Mountain have elevated $\delta^{87}Sr_t$ values compared to samples from the Striped Hills, Specter Range, Spring Mountains, and mountain ranges east of the NTS (fig. 12). These anomalous $\delta^{87}Sr_t$ values were obtained on samples from mineralized areas including the Stirling Gold Mine on the eastern flank of Bare Mountain. Peterman and others (1994, p. 1,321) postulated that hydrothermal mineralization was associated with Tertiary volcanic activity and involved localized plumes of thermal solutions which introduced radiogenic Sr derived from the Precambrian basement into carbonate rocks present at shallower crustal levels. Therefore, the spatial distribution of Paleozoic carbonate rocks with nonmarine $^{87}Sr/^{86}Sr$ compositions at and around the NTS (fig. 12) could be related to major crustal structures that provide fluid pathways and magmatic activity that provided thermal sources.

Paleozoic carbonates present in the northeastern part of the NTS have the potential to be affected by Tertiary magmatic activity constituting the southwestern Nevada volcanic field centered at Timber Mountain and Pahute Mesa (Byers and others, 1989; Sawyer and others, 1994). Results from this study indicate that Paleozoic limestone and dolomite beneath Rainier Mesa, Yucca Flat, and Frenchman Flat tend to have $\delta^{87}Sr_t$ values intermediately between those measured at Bare Mountain and ranges southeast of the NTS (fig. 1; fig. 12A). Carbonate rocks with elevated $\delta^{87}Sr_t$ are present near the bottom of borehole UE-15d (Rainstorm Member of the Johnnie Formation or Noonday Dolomite) underlying a thick section of Neoproterozoic siliciclastic rocks constituting the Lower Clastic Confining Unit in northern Yucca Flat. In western Yucca Flat and the Calico Hills, boreholes ER-16-1, ER-12-1, ER-6-2, UE-16d, and UE-25 a#3 penetrate thick sections of Eleana Formation, Gap Wash Formation, and Chainman Shale consisting of abundant litharenite, siltstone, and shale (fig. 1; fig. 12B). Clay minerals with elevated

Rb/Sr in these siliciclastic rocks constituting the upper clastic confining unit are a possible source for radiogenic Sr in carbonate rocks present in these boreholes. Rocks constituting the upper clastic confining unit are not present in eastern Yucca Flat or Frenchman Flat, and carbonates from ER-3-1, ER-7-1, ER-6-1#2, and HTH #3 have retained their Paleozoic seawater signatures (fig. 12B). Other boreholes having LCA rocks directly underlying Tertiary volcanic or alluvial rocks may or may not have Paleozoic carbonate with elevated $\delta^{87}Sr_t$ values.

In several cases, Sr isotopic compositions were obtained from macroscopically unaltered and altered core samples [Army 1(859) and Army 1(862), TW-C(1458) and TW-C(1463.5)]. For both pairs, samples with brecciated textures, iron staining, and clay mineralization (table 3) had higher $^{87}Sr/^{86}Sr$ values than the sample lacking obvious alteration (table 5). The difference is most dramatic for leachates of samples Army 1(859) and Army 1(862) where the highly altered dolomite has Sr concentrations more than twice the value present in the unaltered dolomite and a $\delta^{87}Sr_t$ value of 3.84 compared to the near seawater value of -0.06 in the unaltered dolomite. Differences are not as large between samples TW-C(1458) and TW-C(1463.5) with negligibly higher Sr concentrations in the altered limestone (261 compared to 251 μg/g) and $\delta^{87}Sr_t$ values of 2.82 compared to 1.87. However, addition of radiogenic ^{87}Sr is not always accompanied by obvious evidence for secondary alteration. Samples UE15d(5994), ER12-4(2580), ER6-2(1830), and ER5-3#2(4780) have $\delta^{87}Sr_t$ values between 3.45 and 5.78, but do not show obvious macroscopic evidence of alteration.

Finally, one pair of samples representing unaltered host dolomite [Army 1(982)A] and coarse secondary dolomite spar [Army 1(982)B] filling a cross-cutting vein were analyzed to investigate the degree of isotopic disequilibrium between the two materials. Leachates of both samples have similar Sr concentrations (30.7 compared to 37.9 μg/g; table 5) and analytically indistinguishable $^{87}Sr/^{86}Sr$ values (0.71027 compared to 0.71023). These data are consistent with a local source of Sr for the younger dolomite spar. Although the age and petrogenesis of the secondary dolomite vein are not known, the thick filling of dense, coarsely crystalline dolomite is not likely to have formed under modern ground-water flow conditions.
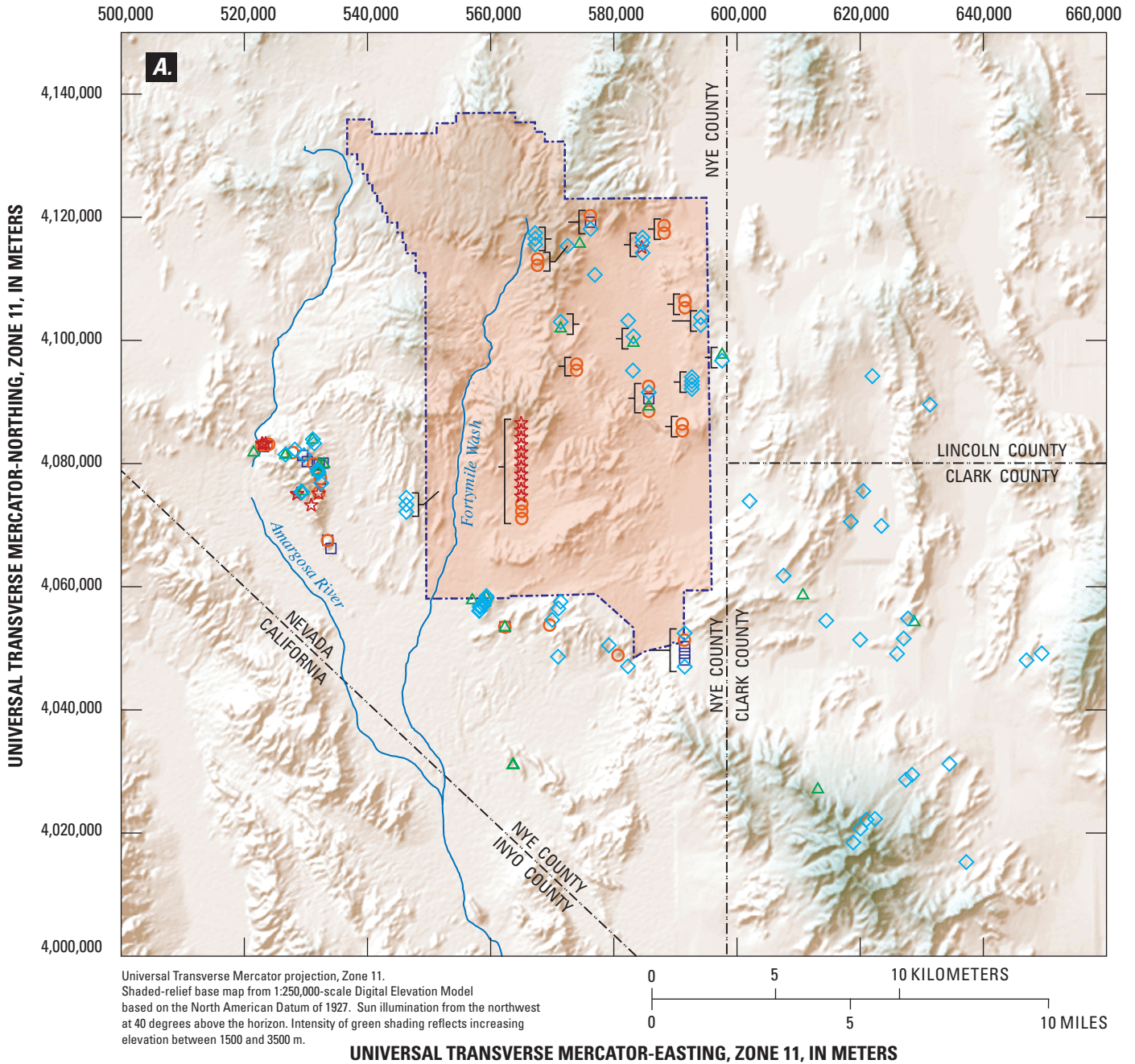
Figure 12. Spatial distribution of $\delta^{87}Sr_t$ values for borehole and outcrop samples (*A*) from the Nevada Test Site vicinity, and (*B*) in and adjacent to the eastern part of the Nevada Test Site, Clark, Lincoln, and Nye Counties, Nevada, and Inyo County, California. Multiple samples from boreholes are shown as vertical arrays in order of depth within borehole (not to scale) with a leader indicating borehole location.
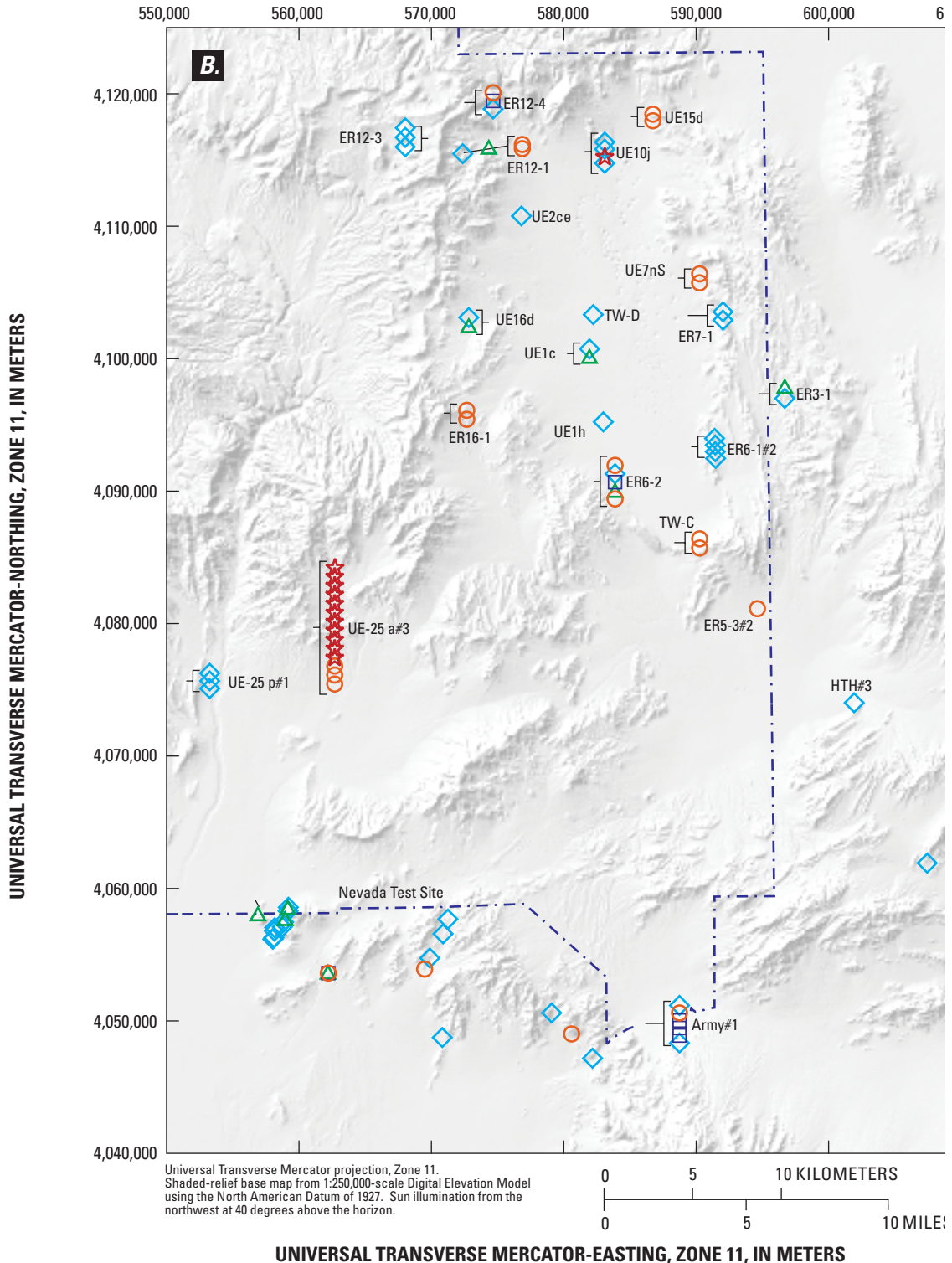
Figure 12.   Continued.

Summary and Conclusions

To contribute to a more accurate understanding of regional ground-water flow beneath the Nevada Test Site vicinity in southern Nevada using $^{87}Sr/^{86}Sr$ values, chemical and strontium isotope data are reported for rock samples representing water-producing horizons in the lower carbonate aquifer, as well as in the upper carbonate aquifer and lower clastic confining unit. Samples obtained in 2006 include core and cutting fragments from 20 boreholes located around Yucca Flat, Frenchman Flat, Rainier Mesa, and Mercury Valley. Partial digestions using dilute nitric acid were used to quantify MgO, CaO, SiO_2, Al_2O_3, MnO, Rb, Sr, Th, and U concentrations in carbonate fractions, which constituted more than 90 percent of most rocks. Small amounts of SiO_2 and Al_2O_3 in leachates are evidence that clay minerals may be present in many carbonate samples. Three samples containing visible shale or volcanic components have SiO_2 concentrations as high as 5–10 weight percent. Dolomites have median Sr concentrations of 46.5 micrograms per gram (µg/g), substantially lower than the median value of 384.5 µg/g for limestones. Because both rock types have similar Rb concentrations, dolomites tend to have higher Rb/Sr ratios. However, these values are low enough in most samples so that increases in $^{87}Sr/^{86}Sr$ caused by decay of ^{87}Rb are not substantial. Values of $^{87}Sr/^{86}Sr$ analyzed from the same leachates of dolomites and limestones range from 0.70809 to 0.72089 and show no dependency on Sr concentrations.

In addition to subsurface samples from NTS boreholes, 114 samples from outcrop, road cut, and underground exposures of Paleozoic carbonates were collected and analyzed in the early-to-mid 1990s. These samples are from locations to the west, south, and east of the NTS including sites in the Funeral Mountains, Bare Mountain, Striped Hills, Specter Range, Spring Mountains, and ranges east of the NTS. Although results for these samples were discussed earlier (Peterman and others, 1994), the data have not been published. Like the borehole samples, dolomite tends to have lower bulk-rock Sr concentrations (typically 22–96 µg/g), whereas limestone tends to have higher Sr concentrations that commonly range up to about 500 µg/g.

The distribution of Sr isotopic compositions from carbonate fractions of borehole and outcrop samples are skewed toward higher $^{87}Sr/^{86}Sr$ values. Many samples have $^{87}Sr/^{86}Sr$ values consistent with Paleozoic seawater $^{87}Sr/^{86}Sr$ values ranging from about 0.7070 to 0.7092. Samples with $^{87}Sr/^{86}Sr$ values greater than 0.7093 have experienced post-depositional modification, which was caused by interaction with fluids containing radiogenic Sr. Carbonate rocks with modified $^{87}Sr/^{86}Sr$ values are present throughout the stratigraphic section. However, rocks with elevated $^{87}Sr/^{86}Sr$ are most common around areas of known mineralization at Bare Mountain, and in western Yucca Flat where the upper clastic confining unit may contribute radiogenic Sr from clay minerals with elevated Rb/Sr. Paleozoic carbonate rocks with

non-marine $^{87}Sr/^{86}Sr$ signatures may show mineralogical or textural evidence of alteration; however, some samples with elevated $^{87}Sr/^{86}Sr$ show no obvious signs of post-depositional modification. The ranges of Sr concentrations and $^{87}Sr/^{86}Sr$ values presented in this report can be used in hydrochemical modeling efforts to represent the composition of carbonate rock dissolved during regional ground-water flow.

Acknowledgments

References Cited

Banner, J.L., 2004, Radiogenic isotopes: systematics and applications to earth surface processes and chemical stratigraphy: Earth-Science Reviews, v. 65, p. 141–194.

Banner, J.L., Wasserburg, G.J., Dobson, P.F., Carpenter, A.B., and Moore, C.H., 1989, Isotopic and trace element constraints on the origin and evolution of saline ground waters from central Missouri: Geochimica et Cosmochimica Acta, v. 53, p. 383–398.

Barnes, Harley, and Christiansen, R.L., 1967, Cambrian and Precambrian rocks of the Groom District, Nevada, southern Great Basin: U.S. Geological Survey Bulletin 1244-G, 34 p.

Burchfiel, B.C., 1964, Precambrian and Paleozoic stratigraphy of Specter Range quadrangle, Nye County, Nevada: American Association of Petroleum Geologists Bulletin, v. 48, p. 43–67.

Burke, W.H., Denison, R.E., Hetherington, E.A., Koepnick, R.B., Nelson, N.F., and Otto, J.B., 1982, Variation of seawater $^{87}Sr/^{86}Sr$ throughout Phanerozoic time: Geology, v. 10, p. 516–519.

Byers, F.M., Jr., Carr, W.J., and Orkild, P.P., 1989, Volcanic centers of southwestern Nevada — Evolution of understanding, 1960–1988: Journal of Geophysical Research, v. 94, p. 5,908–5,924.

Carr, M.D., Waddel, S.J., Vick, G.S., Stock, J.M., Monsen, S.A., Harris, A.G., Cork, B.W., and Byers Jr., F.M., 1986, Geology of drill hole UE25p#1: A test hole into pre-Tertiary rocks near Yucca Mountain, southern Nevada: U.S. Geological Survey Open-File Report 86-175, 87 p.

Chaudhuri, S., Broedel, V., and Clauer, N., 1987, Strontium isotopic evolution of oil-field waters from carbonate reservoir rocks in Brindley field, central Kansas, U.S.A.: Geochimica et Cosmochimica Acta, v. 51, p. 45–53.

Cole, J.C., and Cashman, P.H., 1998, Geologic map of Paleozoic rocks in the Calico Hills, Nevada Test Site, southern Nevada: U.S. Geological Survey Open-File Report 98-101, 19 p.

Cole, J.C., and Cashman, P.H., 1999, Structural relationships of pre-Tertiary rocks in the Nevada Test Site region, southern Nevada: U.S. Geological Survey Professional Paper 1607, 39 p.

Cole, J.C., Harris, A.G., and Wahl, R.R., 1997, Sub-crop geologic map of pre-Tertiary rocks in the Yucca Flat and northern Frenchman Flat areas, Nevada Test Site, southern Nevada: U.S. Geological Survey Open-File Report 97–678, 24 p.

Elderfield, H., 1986, Strontium isotope stratigraphy: Palaeogeography, Palaeoclimatology, Palaeoecology, v. 57, p. 71–90.

Farnham, I.M., Rose, T.P., Kwicklis, E.M., Hershey, R.L., and Paces, J.B., 2006, Geochemical and isotopic evaluation of groundwater movement in corrective action unit 97: Yucca Flat/Climax Mine, Nevada Test Site, Nevada: Stoller-Navarro Joint Venture, Report S-N/99205-070 to DOE, Stoller-Navarro Joint Venture, Las Vegas, Nevada, 283 p. Accessed at http://www.osti.gov/bridge/servlets/purl/877252-NKdprN/877252.PDF on March 14, 2007.

Faure, Gunter, 1986, Principles of isotope geology, (2nd. ed.): John Wiley & Sons, New York, 589 p.

Faure, Gunter, and Mensing, T.M., 2005, Isotopes: Principles and applications (3rd ed.): Hoboken, New Jersey, John Wiley & Sons, Inc., 897 p.

Frost, C.D., and Toner, R.N., 2004, Strontium isotopic identification of water-rock interaction and ground-water mixing: Groundwater, v. 42, p. 418–432.

Gaines, R.V., Skinner, H.C.W., Foord, E.E., Mason, B., and Rosenzweig, A., 1997, Dana's new mineralogy: New York, John Wiley & Sons, Inc., 1,819 p.

Hershey, R.L., Thomas, J.M., Rose, T.P., Paces, J.B., Farnham, I.M., and Benedict Jr., F.C., 2005, Evaluation groundwater movement in the Frenchman Flat CAU using geochemical and isotopic analysis: Desert Research Institute Publication No. 45207, DOE/NV/13609-36: Prepared for the U.S. Department of Energy, National Nuclear Security Administration, Nevada Site Office, Las Vegas, Nevada: Desert Research Institute, 75 p., accessed March 14, 2007, at http://www.osti.gov/bridge/servlets/purl/839138-F6w01Y/native/839138.pdf.

Johnson, T.M., and DePaolo, D.J., 1994, Interpretation of isotopic data in groundwater-rock systems: Model development and application to Sr isotope data from Yucca Mountain: Water Resources Research, v. 30, p. 1,571–1,587.

Johnson, T.M., and DePaolo, D.J., 1997, Rapid exchange effects on isotope ratios in groundwater systems 1. Development of a transport-dissolution-exchange model: Water Resources Research, v. 33, p. 187–195.

Johnson, T.M., Roback, R.C., McLing, T.L., Bullen, T.D., DePaolo D.J., Doughty, C., Hunt, R.J., Smith, R.W., Cecil, L.D., and Murrell, M.T., 2000, Groundwater "fast paths" in the Snake River Plain aquifer: Radiogenic isotope ratios as natural groundwater tracers: Geology, v. 28, p. 871–874.

Laczniak, R.J., Cole, J.C., Sawyer, D.A., and Trudeau, D.A., 1996, Summary of hydrogeologic controls on ground-water flow at the Nevada Test Site, Nye County, Nevada: U.S. Geological Survey Water-Resources Investigations Report 96-4109, 59 p.

Ludwig, K.R., Halley, R.B., Simmons, K.R., and Peterman, Z.E., 1988, Strontium-isotope stratigraphy of Enewetak Atoll: Geology, v. 16, p. 173–177.

Maldonado, Florian, Muller, D.C., and Morrison, J.N., 1979, Preliminary geologic and geophysical data of the UE25a-3 exploratory drill hole, Nevada Test Site, Nevada: U.S. Geological Survey-1543-6, 43 p.

McArthur, J.M., Howarth, R.J., and Bailey, T.R., 2001, Strontium isotope stratigraphy: LOWESS Version 3: Best fit to the marine Sr-isotope curve for 0-509 Ma and accompanying look-up table for deriving numerical age: Journal of Geology, v. 109, p. 155–170.

McKelvey, B.A., and Orians, K.J., 1993, Dissolved zirconium in the North Pacific Ocean: Geochimica et Cosmochimica Acta, v. 57, p. 3,801–3,805.

McKenna, C.M., McNutt, R.H., and Frape, S.K., 1992, Lead and strontium isotopic data on brines from the Michigan basin, Ontario and Michigan *in*, Karaka, Y.K., and Maest, A.S., (eds.), Water-Rock Interaction: Proceedings of the 7th International Symposium on Water-Rock Interaction, Park City, Utah, July 13–18, 1992, p. 971–974.

McNutt, R.H., 2000, Strontium isotopes *in* Cook, P.G., and Herczeg, A.L., (eds.), Environmental tracers in subsurface hydrology: Boston, Kluwer Academic Publishers, p. 233–260.

Monsen, S.A., Carr, M.D., Reheis, M.C., and Orkild, P.P., 1992, Geologic map of Bare Mountain, Nye County, Nevada: U.S. Geological Survey Miscellaneous-Investigations Series Map I-2201, 6 p., 1 sheet.

Page, W.R., Lundstrom, S.C., Harris, A.G., Langenheim, V.E., Workman, J.B., Mahan, S.A., Paces, J.B., Dixon, G.L., Rowley, P.D., Burchfiel, B.C., Bell, J.W., and Smith, E.I., 2005, Geologic and geophysical maps of the Las Vegas 30' x 60' quadrangle, Clark and Nye Counties, Nevada, and Inyo County, California: U.S. Geological Survey Scientific-Investigations Map 2814, 58 p., 2 sheets.

Peterman, Z.E., Hedge, C.E., and Tourtelot, H.A., 1970, Isotopic composition of strontium in seawater throughout Phanerozoic time: Geochimica et Cosmochimica Acta, v. 34, p. 105–120.

Peterman, Z.E., and Stuckless, J.S., 1992, Application of strontium and other radiogenic tracer isotopes to paleohydrologic studies *in* Paleohydrological methods and their applications: Proceedings of an NEA Workshop, Paris, France, November 9–10, 1992, Nuclear Energy Agency, Organization for Economic Co-Operation and Development, p. 59–84.

Peterman, Z.E., Stuckless, J.S., Mahan, S.A., Marshall, B.D., Gutentag, E.D., and Downey, J.S., 1992, Strontium isotope characterization of the Ash Meadows ground-water system, southern Nevada, USA *in* Karaka, Y.K., and Maest, A.S., (eds.), Water-Rock Interaction: Proceedings of the 7th International Symposium on Water-Rock Interaction, Park City, Utah, July 13–18, 1992, p. 825-829.

Peterman, Z.E., Widmann, B.L., Marshall, B.D., Aleinikoff, J.N., Futa, K., and Mahan, S.A., 1994, Isotopic tracers of gold deposition in Paleozoic limestones, southern Nevada: Proceedings of the Fifth Annual International Conference, High-Level Radioactive Waste Management, Las Vegas, Nevada, May 22–26, 1994, American Nuclear Society, LaGrange Park, Illinois, p. 1316–1323.

Poole, F.G., 1974, Flysch deposits of the Antler Foreland Basin, western United States *in* Dickinson, W.R., (ed.), Tectonics and Sedimentation: Society of Economic Paleontologists and Mineralogists Special Publication 22, p. 58–82.

Rose, T.P., Benedict Jr., F.C., Thomas, J.M., Sicke, W.S., Hershey, R.L., Paces, J.B., Farnham, I.M., and Peterman, Z.E., 2006, Geochemical data analysis and interpretation of the Pahute Mesa-Oasis Valley Groundwater Flow System, Nye County, Nevada, August 2002: U.S. Department of Energy, Lawrence Livermore National Laboratory Report UCRL-TR-224559, 137 p..

Sawyer, D.A., Fleck R.J., Lanphere, M.A., Warren, R.G., and Broxton, D.E., 1994, Episodic volcanism in the Miocene southwest Nevada volcanic field—Revised stratigraphic framework, $^{40}Ar/^{39}Ar$ geochronology, and implications for magmatism and extension. Geological Society of America Bulletin, v. 106, p. 1,304-1,318.

Slate, J.L., Berry, M.E., Rowley, P.D., Fridrich, C.J., Morgan, K.S., Workman, J.B., Young, O.D., Dixon, G.L., Williams, V.S., McKee, E.H., Ponce, D.A., Hildenbrand, T.G., Swadley, W.C., Lundstrom, S.C., Ekren, E.B., Warren, R.G., Cole, J.C., Fleck, R.J., Lanphere, M.A., Sawyer, D.A., Minor, S.A., Grunwald, D.J., Laczniak, R.J., Menges, C.M., Yount, J.C., and Jayko, A.S., 1999, Digital geologic map of the Nevada Test Site and vicinity, Nye, Lincoln, and Clark Counties, Nevada, and Inyo County, California: U.S. Geological Survey Open-File Report 99-554-A, 56 p.

Stewart, J.H., and Poole, F.G., 1974, Lower Paleozoic and uppermost Precambrian Cordilleran miogeosyncline, Great Basin, western United States *in* Dickinson, W.R., (ed.), Tectonics and Sedimentation: Society of Economic Paleontologists and Mineralogists Special Publication 22, p. 28–57.

Thomas, J.M., Benedict Jr., F.C., Rose, T.P., Hershey, R.L., Paces, J.B., Peterman, Z.E., Farnham, I.M., Johannesson, K.H., Singh, A.K., Stetzenbach, K.J., Hudson, G.B., Kenneally, J.M., Eaton, G.F., and Smith, D.K., 2002, Geochemical and isotopic interpretations of groundwater flow in the Oasis Valley Flow System, Southern Nevada: Desert Research Institute Publication No. 45, 190 p.

Trexler Jr. J.H., Cashman, P.H., Cole, J.C., Snyder, W.S., Tosdal, R.M., and Davydov, V.I., 2003, Widespread effects of middle Mississippian deformation in the Great Basin of western North America: Geological Society of America Bulletin, v. 115, p. 1,278–1,288.

Trexler Jr., J.H., Cole, J.C., and Cashman, P.H., 1996, Middle Devonian-Mississippian stratigraphy on and near the Nevada Test Site—Implications for hydrocarbon potential: American Association of Petroleum Geologists Bulletin, v. 80, p. 1,736–1,762.

U.S. Department of Energy, 1991, Environmental restoration and waste management—Site-specific plan for fiscal years 1992–1996: U.S. Department of Energy, Nevada Operations Office, unnumbered report, 274 p.

U.S. Geological Survey, 2006, Lithologic-description database (webpage and spreadsheet nts_lth_dsc_061127.xls), accessed January 18, 2007, at http://nevada.usgs.gov/mercury/core.html

Veizer, J., Ala, D., Azmy, K., Bruckschen, P., Buhl, D., Bruhn, F., Carden, G.A.F., Diener, A., Ebneth, S., Godderis, Y., Jasper, T., Korte, C., Pawellek, F., Podlaha, O., and Strauss, H., 1999, $^{87}Sr/^{86}Sr$, $\delta^{13}C$ and $\delta^{18}O$ evolution of Phanerozoic seawater: Chemical Geology, v. 161, p. 59–88.

Winograd, I.J., and Thordarson, W., 1975, Hydrogeologic hydrochemical framework, southcentral Great Basin, Nevada–California, with special reference to the Nevada Test Site: U.S. Geological Survey Professional Paper 712–C, 126 p.

Young, G.C., and Laurie, J.R., 1996, An Australian Phanerozic timescale: Oxford University Press, England, 292 p.

USGS

Paces and others

Strontium Isotopic Composition of Paleozoic Carbonate Rocks in the Nevada Test Site Vicinity, Clark, Lincoln, and Nye Counties, Nevada, and Inyo County, California